TARGETING MITOCHONDRIA WITH ANTIBIOTICS AS A MEANS OF OVERCOMING CHEMORESISTANCE IN TRIPLE NEGATIVE BREAST CANCER

by

CEMİLE USLU

Submitted to the Graduate School of Engineering and Natural Sciences in partial fulfillment of the requirements for the degree of Master of Science

Sabanci University

July 2024

CEMİLE USLU 2024 ©
All Rights Reserved

ABSTRACT

TARGETING MITOCHONDRIA WITH ANTIBIOTICS AS A MEANS OF OVERCOMING CHEMORESISTANCE IN TRIPLE NEGATIVE BREAST CANCER

CEMİLE USLU

Molecular Biology, Genetics and Bioengineering,

MSc Thesis July 2024

Thesis Supervisor: Asst. Prof. Alex Lyakhovich

Keywords: TNBC, metastasis, chemoresistance, OXPHOS, antibiotics

Cancer has remained a factor of mortality worldwide for more than half a century. Among many others, breast cancer is the most important cause of death in women. A particular subtype known as triple negative breast cancer (TNBC) is the most aggressive and has the worst clinical prognosis. The absence of estrogen receptors (ER), progesterone receptors (PR) and low expression of human epidermal growth factor receptors (HER2) allows TNBC to avoid hormonal therapy, forcing the search for other anti-cancer therapy approaches. Since cancer patients do not die directly from primary malignant tumors, but from metastasis, which is often accompanied by cancer resistance, efforts need to be

directed specifically at combating the emergence of metastatic disease. In part, the development of metastases is promoted by so-called cancer stem cells (CSCs) and - a subset of cells living in the tumor with a specific microenvironment, which eventually allows such cells to develop progenitors and colonize in distal organs giving metastases. CSCs are slow dividing and therefore resistant to chemotherapy cells, which often leads to tumor recurrence. In addition, a regular course of chemo- or radiotherapy can select a specific population of cancer resistant cells (CRC) that contribute as much to chemoresistance as CSCs. As shown by various studies, drug-resistant cancer cells exhibit higher levels of mitochondrial respiration than sensitive cancer cells, which is often fueled by ATP from mitochondria-driven oxidative phosphorylation (OXPHOS). Recently, it was suggested that OXPHOS inhibitors may resensitize chemoresistant cells to anticancer therapy. Taking into account the endosymbiotic origin of mitochondria from alphaproteobacteria, we attempted to select antibiotics as chemotherapeutic agents that could inhibit OXPHOS in chemoresistant cells. As a model, we used to cisplatin- resistant TNBC cells. Such cells were found to be OXPHOS-dependent an showed higher oxygen consumption rate, higher doubling time, overexpression of stemness markers and higher metastatic potential compared to sensitive counterparts. After analyzing more than 50 antibiotics, two promising drugs (Amoxicillin and Fosmidomycin soidum salt) with higher toxic effects on chemoresistant cancer cells were selected. Those drugs showed suppression of OXPHOS, decrease in metastatic potential and increase in the autophagy in resistant cells. Overall, our results suggest that some bactericidal antibiotics with proven activity against mitochondria may provide an alternative approach to treat patients with chemoresistant tumors.

ÖZET

ÜÇLÜ NEGATİF MEME KANSERİNDE KEMODİRENCİN ANTİBİYOTİKLERLE MİTOKONDRİNİN HEDEFLEMESİ YOLUYLA AŞILMASI

CEMİLE USLU

Moleküler Biyoloji, Genetik ve Biyomühendislik,

Yüksek Lisans Tezi, 2024

Tez Danışmanı: Doktor Öğretim Üyesi. Alex Lyakhovich

Anahtar Kelimeler: TNBC, metastaz, kemodirenç, OXPHOS, antibiyotikler

Kanser yarım yüzyıldan fazla bir süredir dünya çapında önemli bir ölüm nedeni olmaya devam etmektedir. Diğer türlerin yanısıra meme kanseri kadınlarda en önemli ölüm nedenidir. Üçlü negatif meme kanseri (TNBC) olarak bilinen meme kanseri türü, en agresif olan alt tiptir. Östrojen ve progesteron reseptörlerinin sentezlenmemesi ve epidermal büyüme faktörü reseptörlerinin düşük ekspresyonu, TNBC'nin hormonal tedaviden kaçınmasına olanak tanıyarak diğer kanser karşıtı tedavi yaklaşımlarının araştırılmasını mecbur kılmaktadır. Kanser hastaları doğrudan birincil kötü huylu tümörlerden ziyade, sıklıkla kanser direncinin eşlik ettiği metastazdan hayatlarını

kaybetmektedirler. Bu yüzden tedavi çabalarının özellikle metastatik hastalığın ortaya çıkışıyla mücadeleye yönlendirilmesi gerekmektedir. Metastaz, kanser kök hücreleri (CSC'ler) adı verilen, tümör içindeki belirli alt küme hücreleri tarafından tetiklenmektedir. Bu, sonunda bu tür hücrelerin progenitörler geliştirmesine ve metastaz yaparak diğer organlarda kolonileşmesine sebep olmaktadır. CSC'ler yavaş bölenen ve bu nedenle kemoterapiye karşı dirençli hücrelerdir. Bu durum sıklıkla tümörün nüksetmesine yol açmaktadır. Ek olarak, düzenli bir kemoterapi veya radyoterapi tedavisi, CSC'ler kadar ilaç direncine katkıda bulunan, kansere dirençli hücrelerini (CRC'ler) ortaya çıkarabilir. Çeşitli çalışmalarda da gösterildiği üzere, ilaca dirençli kanser hücrelerinin enerji mekanizması, hassas kanser hücrelerine göre daha fazla mitokondriyel oksidatif fosforilasyona (OXPHOS) dayanmaktadır. Son zamanlarda yapılan çalışmalarla OXPHOS inhibitörlerinin dirençli kanser hücrelerini antikanser tedavisine yeniden duyarlı hale getirebileceğini öne sürüldü. Bu çalışmada mitokondrinin alfaproteobakterilerden olan endosimbiyotik kökenini de dikkate alarak, bakterisidal ilaçları, dirençli kanser hücrelerinde OXPHOS'u inhibe edebilen kemoterapötik ajanlar olarak seçtik. Model olarak sisplatine dirençli TNBC hücrelerini kullandık. Bu tür hücrelerin OXPHOS'a bağımlı olduğu ve hassas kanser hücrelerine kıyasla daha yüksek oksijen tüketim oranına, daha yüksek büyüme süresine ve daha yüksek metastatik potansiyeline sahip olduğunu gösterdik. 50'den fazla antibiyotiğin analiz edilmesinin ardından, ilaca dirençli kanser hücreleri üzerinde daha yüksek toksik etkiye sahip iki ilaç (Amoksillin-Amx ve Fosmidomisin sodyum tuzu-FSS) seçildi. Bu ilaçların dirençli hücrelerde OXPHOS'u inhibe ettiğini, hücrelerin metastatik potansiyelini düşürdüğünü ve otofajiyi artırdığını gözlemledik. Genel olarak sonuçlarımız, mitokondriye karşı kanıtlanmış aktiviteye sahip bazı bakterisidal antibiyotiklerin, ilaç direnci kazanmış tümörleri olan hastaların tedavisinde alternatif bir yaklaşım sağlayabileceğini göstermektedir.

ACKNOWLEDGEMENTS

First of all sentences I would like to express my sincere thanks to my supervisor Asst. Prof. Alex Lyakhovich for his limitless support, extensive knowledge, patient and understanding. It was a great opportunity for me to work under his supervision and learn from his experiences. He was always willing to teach me the best of his knowledge even in his busy times.

I also want to express my acknowledgement to TUBITAK as being financial supporter of the project entitled "Mitochondrial-dysfunction inducing antibiotics as the novel chemotherapeutic agents against cancer chemoresistance" number:121C096.

I would like to thank my family, my father and my mother who are always there for me and for believing me and supporting me. Additionally I feel myself lucky to have my close friends Aybüke Büşra Özer, Büşra Elif Kıvrak, Gülnur Şener, Gülşah Yıldız, Sümeyye Narin and Ahmet Baki Şahin as being like my second family in Sabanci University and make this master journey bearable for me.

To my future self, my future children,

my family and peaceful World…

TABLE OF CONTENTS

LIST OF FIGURES

LIST OF TABLES

LIST OF ABBREVIATIONS

Ab Antibody

ABC transporters ATP binding cassette (ABC) transporters

ADP Adenosine-5'-Diphosphate

Amx Amoxicillin (sodium)

bFGF Basic Fibroblast Growth Factor

CRCs Cancer Resistant Cells

CSCs Cancer Stem Cells

CTCs Circulating Tumor Cells

DCIS Ductal Carcinoma in Situ

DMEM Dulbecco's Modified Eagles Medium

EMT Epithelial to Mesenchymal Transition

ER Estrogen Receptor

ETC Electron Transport Chain

FBS Fetal Bovine Serum

FCCP Carbonyl cyanide-p-trifluoromethoxyphenylhydrazone

FSS Fosmidomycin Sodium Salt

H+ Proton

HER2 Human Epidermal Growth Factor Receptor

IC Inhibitory Concentration

IDC Invasive Ductal Cell Carcenoma

kDA Kilodalton

MDF Disfunctional Mitochondria

MET Mesenchymal to Epithelial Transition

mM Millimolar

MMP-2 Matrix Metalloproteinases 2 (Gelatinase A)

MMP-9 Matrix Metalloproteinases 9 (Gelatinase B)

MMPs Matrix Metalloproteinases

mtDNA Mitochondrial DNA

MTT (3-(4,5-dimethylthiazol-2-yl)-2,5-diphenyl tetrazolium bromide)

nM Nanomolar

OCR Oxygen Consumption Rate

OXPHOS Oxidative Phosphorylation

P Parental (sensitive) MDA MB 231 cells

P+Amx Parental MDA MB 231 cells treated with Amoxicillin (sodium)

P+FSS Parental MDA MB 231 cells treated with Fosmidomycin Sodium Salt

PR Progesterone Receptors

PVDF Polyvinylidene Fluoride

R Cisplatin resistant MDA MB 231 cells

R+Amx Resistant MDA MB 231 cells treated with Amoxicillin (sodium)

R+FSS Resistant MDA MB 231 cells treated with Fosmidomycin Sodium Salt

ROS Reactive Oxygen Species

RT-q PCR Real Time Quantitative PCR

SDS Sodium Dodecyl Sulfate

TICs Tumor Initiating Cells

TNBC Triple Negative Breast Cancer

uM Micromolar

1. INTRODUCTION

Cancer has held a steady place on the podium of human mortality over the past half century and this trend is only set to accelerate over the next (Bray Bsc et al. 2024). This is partly because the world's population is aging and we are more likely to live to see “our cancer” and partly because of advances in diagnostic technology, which is now detecting many more cases of cancer than it did a decade ago (WHO 2020). It is generally accepted that cancer represents not one, but many different diseases united under the umbrella of a couple of important properties of the cell - uncontrolled division and immortality (National Institutes of Health 2007). Since the spectrum of genetic mutations combining these two properties varies greatly from tissue to tissue, from organ to organ, we end up with hundreds of different phenotypic manifestations resulting in what is called a malignant tumor (Mendiratta et al. 2021).

All malignant tumors are conditionally divided into different types, of which cancer is a malignancy deriving from epithelial tissues (Méndez-López 2022). Further, depending on the type of organ, such tumors are divided into the corresponding type including liver, breast, kidney, lung, stomach and many other types of cancers. It is important to understand that not all cancers have the same properties, the same evolution and the same prognosis to treatment – this is mainly dependent on genetic and epigenetic mutations, tumor microenvironmen and the rate at which certain cancer cells can devide. Among cancers with rapidly dividing cells, breast cancer is one of the most lethal (Orrantia-Borunda et al. 2022)

Breast cancer has the most leading cause of death among all women cancers worldwide (Orrantia-Borunda et al. 2022; Siegel, Giaquinto, and Jemal 2024). Most breast cancers (carcinomas or malignant breast tumors) start in the epithelial cells that line organs and tissues throughout the body (Méndez-López 2022). When carcinomas form in the breast, they are usually called adenocarcinoma, which starts in cells in the ducts or the lobules (Del Pino Herrera and Ferrall-Fairbanks 2024). Breast cancer can also refer to whether the cancer has spread. For instance, ductal carcinoma in situ (DCIS) is a benign or a pre-cancer that starts in a milk duct and has not expand to the other part of the the breast tissue

(Delaloge et al. 2024). In turn, invasive ductal cell carcenoma (IDC) describes a type of breast cancer that has invaded into the surrounding breast tissue. It is the most common type of breast cancer (80% of all cases)(Arps et al. 2013).

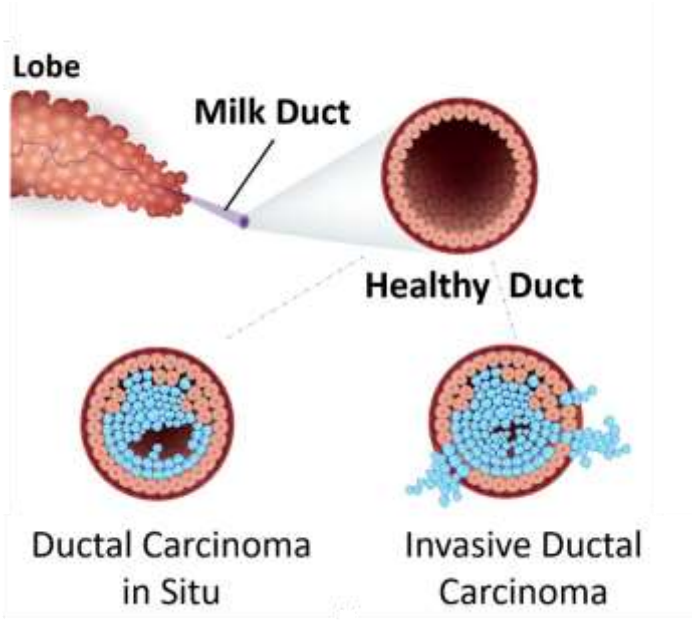

Figure 1. Representative images of Ductal carcinoma types. Ductal carcinoma in situ (DCIS) is benign and do not metastasize while invasive ductal carcinoma is aggressive and invades other tissues (Understanding Breast Cancer Types | Colorado's Breast Cancer Specialists n.d. (https://www.rockymountaincancercenters.com/breast-cancer/types-hormone-receptors)

1.1. Triple Negative Breast Cancer

Due to the progress made in molecular oncology and in the diagnostics of malignant tumors it became possible to further characterize breast cancers by the type of molecular signatures or surface receptors attributed to specific types of breast cancers which has a heterogeneous nature and now include at least 4 different subtypes (Shaath, Elango, and Alajez 2021). These subtypes are categorized upon involvement of estrogen receptors (ER), progesterone receptors (PR) and or the presence or absence of human epidermal growth factor receptors (HER2+ or HER2-). (Irvin and Carey 2008). Based on these features triple-negative breast cancer (TNBC) refers to the fact that the cancer cells

do not have ER and PR, and have very low expression of HER. TNBC accounts for about 20% of all breast cancers and tend to be more common in younger women, or who have a BRCA1 mutation (Orrantia-Borunda et al. 2022). TNBC differs from other types of invasive breast cancer as it grows and spread faster.

Unlike other common breast cancers which can be treated with hormone therapy due to the presence of surface receptors (ER+, PR+ or HER2+ types of breast cancers) or by blocking corresponding growth factors and inhibiting the cell-cell communication and cell growth. TNBC lacks such receptors (Wolff et al. 2018) and therefore is insensitive to endocrine therapy. Not surprisingly, TNBC demonstrating very aggressive character has the worse clinical prognosis (Orrantia-Borunda et al. 2022; Yin et al. 2020).

1.2. Metastasis and Cancer Stem Cells

It is a stereotype of people to think that oncological patients die from cancer (or malignant tumor in a common term). In fact, the most deaths in the cancer patients is not a result of primary tumor but the metastasis, - dissemination of cells from primary tumor origin to distant organs (Gerstberger, Jiang, and Ganesh 2023). Metastasis is a dynamic process in which overlapping steps are involved: dissemination, dormancy and colonization (Massagué and Ganesh 2021). This is mainly taking place due to clonogenic selection of primary tumors that give rise to a more aggressive and more metastatic clones due to high mutation rate of cancers undergoing selection by microenvironmental factors or during the course of chemo-, radio- or immunotherapy (Testa, Castelli, and Pelosi 2019).

There are different ways metastasis can occur. One of them is when metastatic cells in primary tumors gain mobility through so-called epithelial to mesenchymal transition (EMT) (Yang et al. 2020). This process may involve gaining novel mutations in the primary tumor or activate epigenetic program to activate expression of genes responsible for the tumor cell to detach from its origin. This includes expression and activation of matrix metalloproteinases (MMPs), enzymes that enable to digest surrounding stromal tissues scaffolding primary tumor and form so-called circulating tumor cells (CTCs). CTC's have low adhesion and high migration capacities and may penetrate to the

bloodstream or lymphatic system to travelling into the distant organs where they have to convert EMT to its opposite counterpart: mesenchymal to epithelial transition (MET) enabling such cells to envade, re-gain adhesion properties and form a new clone (metastasis) (Hanahan and Weinberg 2011).

It is suggested that only a small population of tumor cells often result in metastasis (Talmadge and Fidler 2010a). These cells could be therapy-evolved and selected from the primary pool of cancer cells due to mutations or they could be a special subset of cells called cancer stem cells (CSCs). Such cells, also having EMT program, in adition have stem cell properties which makes them be more resistant to anticancer treatment (Batlle and Clevers 2017). CSCs not only play role in metastasis but can be also active tumor initiators helping it to develop and progress (Su et al. 2021). In the literature these cells also exist under the name of tumor initiating cells (TICs) or side-populated cancer cells. Since CSCs are resistant to therapy, they can survive in the tissue even if the main tumor is removed via chemo- or radiotherapy or surgery (Shibata and Hoque 2019). CSCs can be identified by specific biomarkers of stemness which are also used as prognostic markers for aggressiveness of the cancer (Phi et al. 2018). For example, in breast cancer, CD24, CD29, CD44, CD44f, CD61, CD70, CD90, CD133, CXCR4, EpCAM, LGR5, pROC-R, ALDH, Nanog, Notch, SOX2, Oct-3/4, BMI-1 are the markers used for characterization of the CSCs (Walcher et al. 2020). Activation of common tumorigenic pathways, e.g. adhesion pathway or Wnt/B-catenin pathway, may also serve as a marker associated with stemness (Schwitalla et al. 2013).

1.3. Tumor Relapse and Cancer Resistance

It is believed that stemness is one of the reasons for tumor relapse and metastasis (Luo, Brooks, and Wicha 2015). Many studies have been investigated why and how does tumor become recurrent and give rise to metastasis and why after successfull medical interventions many malignant tumors become resistance to such therapy (Figure 2). One of the reasons could be cancer residual disease which is often linked to the presence of CSCs. In addition to CSC's, another subpopulation of tumor cells called cancer resistant cells (CRC) play an active role in tumor recurrence and occasionaly used in the name of

CSC's (Talmadge and Fidler 2010b). CSCs may be kept and stored in so-called dormant state of special places in the body protected by microenvironment (metastatic niches) from immune system or from the therapeutic interventions, making them tumor resistant (Plaks, Kong, and Werb 2015). Alternatively, resistant to therapeutic treatment regimen can be created by many other ways, mainly associated with aquisition of additional specific mutations in the primary tumor that allows offspring clones to overcome any type of drug or radiation treatments. Several mechanisms of anticancer drug resistance have been described to this end (Cree and Charlton 2017). One of them is overexpression or high activity of ATP binding cassette (ABC) transporters (Sales Amaral et al. 2019). Superfamily of ABC transporters carries drugs out of cells to decrease drug concentration and allow cells to survive. It is for that reason, that ABC transporter inhibitors have been suggested to overcome drug resistance (Fanelli et al. 2016; Wen et al. 2019).

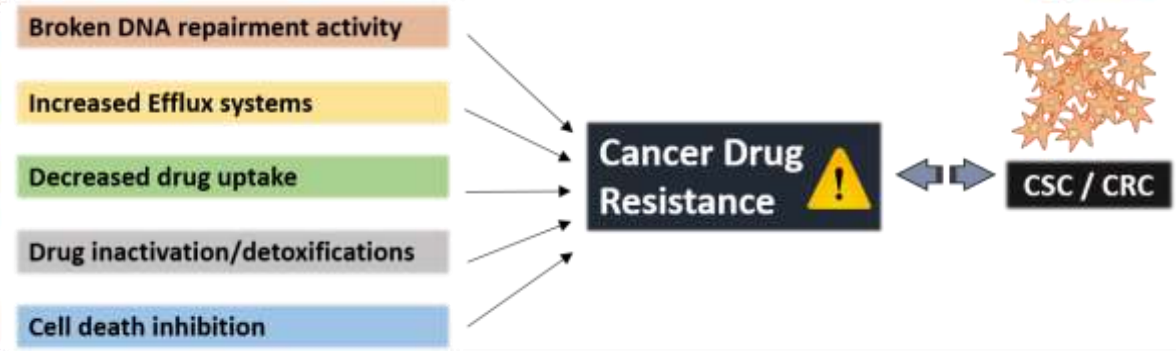

Figure 2. Major drug resistance mechanisms that may lead to recurrence and metastasis of tumor associated with CRC and CSCs. Drug resistance can be developed through enhanced DNA repair mechanisms as well (Mansoori et al. 2017). Many chemotherapeutic drugs, e.g. cisplatin, cause cell death in tumors by binding DNA and forming DNA-drug adducts which disrupts transcription and causes DNA damage (Ghosh 2019). Disrupting the DNA repair activity with various inhibitors can manage the drug resistance (Mansoori et al. 2017). For example, inhibition of poly(ADP-ribose) polymerase 1 (PARP1) enzyme participating in DNA non -homologous end joining repair system and can be alternative anticancer therapy (Q. Wang et al. 2017).

Many other anti cancer drugs acquire activity in vivo after metabolic interaction with other molecules or proteins (Mansoori et al. 2017; Zaal and Berkers 2018). Decreasing

metabolic activity may serve as a way to overcome drug resistance (Michael and Doherty 2005). For instance, the drug cytarabine is only active if it goes through several phosphorylation steps. Cancer cells overcome toxicity to cytarabine by downregulating enzymes in phosphorylation reactions (Sampath et al. 2006). Drug inactivation may take place through detoxification systems (Huang, Xu, and Liu 2015). For example, platinum drugs can be detoxified with metallothionein enzymes (Huang, Xu, and Liu 2015). Glutathione S-transferase family proteins, which play a primary role in drug detoxification, may cause drug resistance by inactivation and/or inhibition of MAPK signaling pathway (Townsend and Tew 2003). Among many other drugs, platinum-containing ones, such as cisplatin, are one of the most frequently used groups of anticancer agents in chemotherapeutic intervention and at the same time the group of drugs that most frequently acquire chemoresistance.

1.4. Cisplatin and its mechanism of action during chemotherapy

Chemotherapy is a frontline neoadjuvant treatment for the TNBC patients (Lebert et al. 2018). Taxane, anthracycline-like and platinum based agents, are frequently used as chemotherapeutic drugs (Lebert et al. 2018). Platinum agents stimulate apoptosis by inhibiting DNA synthesis through forming cross links between DNA and proteins thus interferring with mitotic cells (Bardal, Waechter, and Martin 2011). Cisplatin represents one of these drugsand is used specifically in the treatment of TNBC patients (Hill et al. 2019).

Cisplatin as an anticancer drug was discovered mistakenly by Barnett Rosenberg in 1965 with his experiments on E. coli. Dr. Rosenberg and his group realized that chemical residue in the experimental setup leads bacteria to grow but now divide. After this discovery they developed this Pt-based residue and suggested using it as an anticancer agent (Figure 2). Finally, they synthesized compound named cisplatin and showed that it effectively arrested leukemia and sarcoma cells (Rosenberg et al. 1967). It became the first platinum carrying drug approved by FDA (Kelland 2007), since including heavy metals in the drugs was not certified due to hazard concerns before the 1970s.

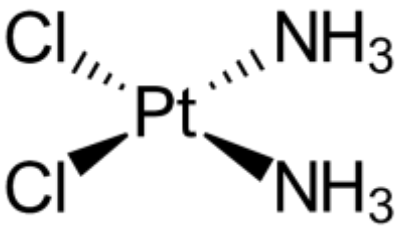

Figure 3. Chemical structure of cisplatin

To exhibit its toxic effect, cisplatin should first enter the cell body. Cisplatin can successfully enter the cells via passive diffusion since it does not carry any charge (Makovec 2019). However, it was also proposed that it can be carried inside the cell via copper transporters (Eljack et al. 2014).

Most prominent mechanism of action of cisplatin is the formation of bifunctional adducts via DNA-cisplatin interactions. Several types of adducts and crosslinks can be formed between cisplatin and DNA (Saad, Najjar, and Alashari 2004). This interaction causes DNA damage and activates apoptosis. Cisplatin also induces formation of reactive oxygen species (ROS) and triggers ROS-dependent apoptosis pathways (Florea and Büsselberg 2011).

Since mitochondria are also a notable target for ROS, respiratory mechanisms may be disrupted by (Ghosh 2019). ROS also lead to mtDNA damage, increase in mitochondrial permeability and rupturing, release of cytochrome c and eventually formation of apoptosome complexes (Green 1998). Cisplatin can also attack other organelles by forming protein adducts (Makovec 2019).

Mitochondria is known as a powerhouse organelle of the eukaryotic cells that is mainly responsible for ATP synthesis with aerobic respiration and energy conversation (Roger, Muñoz-Gómez, and Kamikawa 2017). Although it is mitochondria gets its fame with its role in oxydative phosphorilation (OXPHOS), mitochondria play active role in apoptosis, cellular signaling, production of ROS, oxidation of fatty acids and providing cellular homeostasis as well. (Chinnery 2003; Wallace 2012). This double membraned organelle carries its own circular DNA (mtDNA) which is necessary for encoding 13 proteins. These proteins are components of respiratory complexes (Jang et al. 2018).

1.5. Multiple Roles of Mitochondria in Cancer

Origin of the mitochondria is explained by Endosymbiotic Theory. This theory suggest symbiotic integration of ancient bacteria into proto-eukaryatic host. Roots of this theory was published by Lynn Sagan (Margulis) with the article “On the Origin of Mitosing Cells” in 1967 (Margulis 1967). By coming recent years, with the advances in proteomics and sequencing technologies, it is widely accepted that Alphaproteobacteria is the most close ancestor of the mitochondria (Z. Wang and Wu 2015). Alphaproteobacteria are belong to Pseudomonadota phylum and have gram negative characteristics (Osborne 2008).

ATP is synthesized predominantly through the OXPHOS in the mitochondria. Electron carrying molecules produced in the citric acid cycle are transferred to the electron transport chain (ETC) in the inner membrane of the mitochondria to start OXPHOS. Electrons are transferred down to 4 main (respiratory) protein complexes in ETC to generate proton (H+) gradient. H+ gradient is used by ATP synthase at the last step to synthesize ATP (Xu et al. 2020).

Switching from mitochondria-dependent OXPHOS to glycolysis for ATP production in malignant tumors is known as the “Warburg Effect" dedicated to its discoverer Otto Warburg (Warburg and Minami 1923). It is suggested that resistant cancer cells mostly rely OXPHOS rather than glycolysis as opposed to the classical Warburg effect phenomena observed in regular cancer cells (Lagadinou et al. 2013; Pastò et al. 2014). The same is true for the CSCs which seem to rely on OXPHOS rather than glycolysis (Uslu et al, 2024). This status of CRC promises therapeutic approaches which can target bioenergetic mechanisms of resistant tumors.

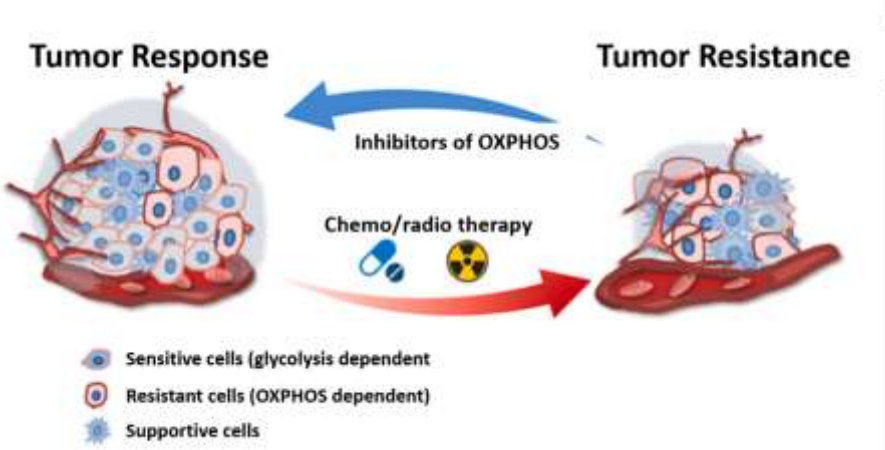

Figure 4. Alteration in the tumor microenvironment following chemotherapy or radiotherapy. Sequential chemotherapy or radiotherapy leads to a shift in the tumor population, where rapidly dividing cancer cells that originally relied on glycolysis develop resistance and transition to a dependency on (OXPHOS) (Uslu, Kapan, and Lyakhovich 2024)

In the study of Evans and colleagues (Evans et al. 2021) anthracycline and taxane-resistant xenograft models taken from TNBC patients demonstrate high OXPHOS level and mitochondrial complex I activity. Moreover, complex I inhibitor IACS-10759 effectively showed antitumor activity in xenograft models. In another study, epirubicin-resistant TNBC cells (MCF-7) demonstrated intense increase in the OXPHOS and mitochondrial metabolism of energy. These cells were also sensitive to PGC-1α (regulator of OXPHOS) knock down (McGuirk et al. 2021).

It was demonstrated in chemoresistant TNBC cells that MCL1 and MYC are highly expressed and this high expression is correlated with increased OXPHOS (Lee et al. 2017) which in turn led to elevated ROS level and HIF-1α expression (Lee et al. 2017). Proteomics studies also showed an association between increased OXPHOS and drug resistance (Anurag et al. 2022).

In cyclophosphamide, cisplatin and doxorubicin resistant TNBC cells it was revealed that mitochondrial activity was increased (Abad et al. 2019). In addition expression of mitochondrial proteins involved in TCA cycle and mitochondrial complexes I and V were higher than in sensitive (parental) TNBC cells (Abad et al. 2019). Since both CRC

and CSCs revealed OXPHOS dependency in drug resistant breast cancer, targeting OXPHOS mechanisms was suggested as a therapeutic approach in the treatment of resistant TNBC. For example, small-molecule inhibitor NSC33353 blocked OXPHOS pathway and resensitized doxorubicin resistant TNBC cells to decrease cell proliferation (Yousefi et al. 2022). A polydrug TF@CNM + DOX that carries doxorubicin and specifically targets mitochondria of chemoresistant TNBC cells inhibited growth of drug resistant tumors (Mukerabigwi et al. 2023).

Recently, we performed a multivariate analysis of breast cancer patients between 2010 and 2021 to demonstrate distict correlation between expression level of OXPHOS related genes and survival rate of the patients (Uslu, Kapan, and Lyakhovich 2024). This analysis reveals that before chemotherapy, patients who have low gene expression of Cytochrome C oxidase (COX 1), - one of the subunits of respiratory complex IV, ATP 6, - one of the subunits of ATP sythase, NDUFA2, - a subunit of ubiquinone, SDH 1, one of the subunits of succinate dehydrogenase, UQCRB, a ubiquinol-cytochrome c reductase binding protein and TCIRG1, vacuolar ATPase, have higher survival rate than patients who have increased expression of same genes. This suggest a poor clinical outcome for the patients whose malignant tumors have active and function mitochondria. In addition, after chemotherapy, patient whose malignant tumors express lower level of OXPHOS genes, have higher survival rates. Overall, these results indicate that after chemotherapy patients, who most likely will develop drug resistance correlating with higher expression of OXPHOS genes, may have poor survival rate. Along with many other previously published results this suggests that targeting mitochondria/OXPHOS can be a promising approach to overcome chemoresistance of some malignant tumors.

Since miitochondria inheriting the traits of alphaproteobacteri can be susceptible to antibactericidal drugs, antibiotics were suggested as an alternative treatment of some cancers. One of the first studies were performed in vitro (Lamb et al. 2015). Lamb and colleagues tested 5 group of antibiotics (erythromycins, the tetracyclines, the glycylcyclines, an anti-parasitic drug, and chloramphenicol) on 12 different cancer cells including breast cancer. All of these antibiotics selectively inhibited tumor-sphere formation, an in vitro emulation of CSCs. Erythromycins and chloramphenicol both inhibited mitochondrial biogenesis by binding larger subunit of mitochondrial ribosome, while tetracyclines and glycylcyclines inhibited it by binding smaller subunits of

mitochondrial ribosome, including translation of OXPHOS proteins (Lamb et al. 2015). We previously suggested that not only antibiotics should be applied to inhibit cancer cell growth but also authophagy should be blocked as it surves as a survıval pathway to clear up dysfunctional mitochondria (MDF) (Esner et al. 2017). Previous studies of the PI's lab proposed that antibiotics inducing MDF can be universaly repurposed and used against some types of cancers (Lleonart et al. 2017). Later, Gottlieb's group first demonstrated on mice that leukemia cells can be suppressed by inhibiting OXPHOS with tetracyclines (Kuntz et al. 2017). In parallel, similar approach on mice carrying TNBC zenographts confirmed these results (Abad et al. 2019). For that reason, we proposed to undertake massive screening of antibiotics which could potentially target mitochondria of resistant forms of cancer.

2. AIM OF THE STUDY

The current study is mainly focused on finding antibiotics that can be repurposed as a novel chemotherapetic agents against chemoresistant TNBC. To this end, the following specific aims were undertaken:

(1) Establish a cisplatin-resistant TNBC model from MDA MB 231 cells and study the divergence between the phenotype of cisplatin-resistant and sensitive (parental) cells;

(2) Screen an antibiotic library over cisplatin-resistant and sensitive cells and select promising antibiotics (leads) that may affect OXPHOS and other pathways to specifically eradicatd chemoresistant TNBC cells;

(3) Explore some of the molecular pathways that may be engaged by the selected antibiotics, with the ultimate goal of modifying such drugs for specific delivery to mitochondria and validating the results of *in vitro* studies in animal experiments. To achieve these aims, the following strategies were undertaken (see scheme of workflow below): (i) antibiotics from a chemical library (<500 compounds) with broad spectrum activity or activity against Gram-negative (Gr-) bacteria were examined. This was done because the mitochondion is a double-walled organell sourced from Gr- bacteria; (ii) in parallel, chemoresistant TNBC cell lines were generated, in particular, cisplatin-resistant MDA MB 231 cells. Other models include tumosphere (mammosphere) cancer stem-like cells (CSCs), as well as the cyclophoshamide –resistant MDA MB 468 TNBC cell line (not shown in the schematic); (iii) preselected antibiotics were applied to both resistant and sensitive (parental) TNBC cells to select a few candidates showing the most significant difference in the survival assay; (iv) pre-selected candidates (leads) were applied to both resistant and sensitive (parental) TNBC cells for validating some of the proposed pathways.

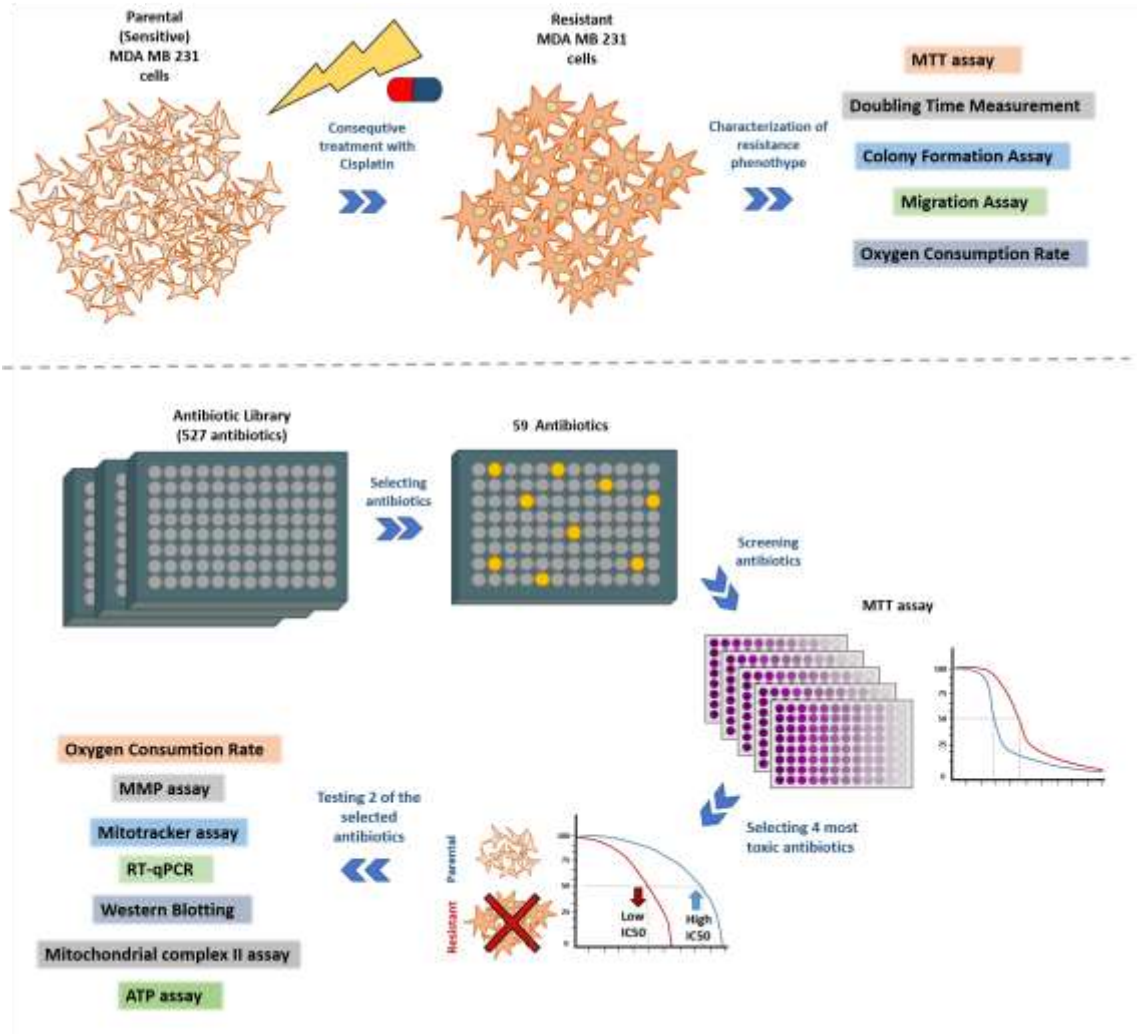

Figure 5. Schematic representation of the study workflow. First, several clones of chemoresistant TNBC cells as well as CSCs (above panel) were generated. MDA MB 231 sensitive (parental) and cisplatin resistant MDA MB 231 cells were selected and characterized in several assays. In parallel, 59 antibiotics were pre-selected from a drug library containing 527 antibiotics and tested by MTT assay on established cell models of parental and resistant cells (central panel). Four drugs (leads) with stronger toxic effects on resistant cells were selected and two of them were further tested in biophysical and biochemical assays (bottom panel). In addition, some specific pathways were confirmed by the corresponding assays.

3. MATERIALS AND METHODS

3.1. Cell Maintenance

Parental (sensitive) MDA MB 231 cells obtained from ATCC collection (www.atcc.org) were grown in complete DMEM (Gibco, US) containing 10% Fetal Bovine Serum (Capricorn Scientific, US) and 1% Penicillin/Streptomycin (Gibco, US).

3.2. Culturing Cancer Stem-like Cells

MDA-MB-231 parental and cisplatin resistant cell lines were used to obtain cancer stem cells (CSC) in the forms of mammosphers. To obtain CSC, a single cell suspension was prepared using enzymatic disaggregation and cells were plated at a density of 10.000 cells per ml in Cancer Stem Cell medium containing bFGF and EGF (10 nM each) in Poly-HEMA (Santa Cruz Biotechnology, Germany) coated plates. The cells were later verified using known stem cell markers by RT-PCR. Cells forming mammosphers of first generations (G1) were used to maintain second (G2) and third (G3) generations, each grown for 5-7 days and used for tumosphere assay.

3.3. RNA Isolation

Nucleogene QuickEX Total RNA isolation kit (Nucelogene, Turkey) was used for RNA isolation from cells representing parental, resistant, stem cells, parental and cisplatin resistant MDA MB 231 cells treated with 790 uM of Amoxicillin (sodium) and 345uM of Fosmidomycin sodium salt for 3 days) collected and counted. Total RNA was isolated from 1×10^6 cells. Briefly, cells were digested with 600 ul Lysis Buffer for 15 minutes at room temperature and centrifuged at 14.000×g for 2 minutes in microcentrifuge

(Eppendorf, Germany). Supernatat was collected and mixed with same volume of pure ethanol (Merck) (400ul supenatant+ 400ul ethanol) and mixed vith vortex for 1 minutes. Solution was transferred to spin column and centrifuged at 11.000×g for 30 seconds in microcentrifuge (Eppendorf, Germany). Collected solvent was discarded. DNase I treatment was done following the instructions of manufacturer. 5uL DNase (6U/I) was mixed with 45 uL of DNase I Buffer and for each group of cells. 50 uL of DNase solution was dropped on matrix column and incubated at room temperature for 15 minutes.

Matrix column washed with 400 ul Wash Buffer I and centrifuged at 11.000×g for 30 seconds two times. Next, matrix column was washed with 700 uL Wash Buffer II and at 11.000×g for 1 minutes. Collection tube was replaced with clean tube and RNA was eluted with 100 uL Elution Buffer by centrifugation at 14.000×g for 2 minutes.

Concentration and purity of isolated RNA was measured by Nanodrop UV/Vis Spectrophotometer (Thermo Scientific NanoDrop 2000, USA). Elution Buffer was used as a blank during measurement.

3.4. cDNA Synthesis

cDNA was synthesized from isolated RNA's for each group of cells with Nucleogene cDNA synthesis Kit (5X) (Nucleogene, Turkey). This kit contains reaction buffer which includes optimized concentrations of dNTP's and $MgCl_2$. cDNA was synthesized from 100 ng RNA for each group of cells. Volume of water were calcultated according to 20 uL final reaction volume after substraction of 100 ng RNA and reaction buffer volumes. Reaction components and incubation conditions was applied as indicated in the tables below. Thermocycler was used for reaction.

Table 1. Components of the cDNA synthesis

Component	**Volume/ Amount**
Reaction Buffer (5X)	4 uL
Water (RNase/DNase free)	Variable
RNA	100 ng
Total volume:	20 uL

Table 2. c DNA reaction conditions

Step	Temperature	Time
1	25 C°	5 minutes
2	50 C°	30 minutes
3	85 C°	5 minutes
4	4 C°	∞

3.5. Real Time Quantitaive PCR (RT-qPCR)

Real time q-PCR reaction was performed for 3 genes (SOX-2 and Nanog) and housekeeping gene (GAPDH). Reaction was performed with 3 replicas for each group of cDNA's. 4 uL cDNA was used in each 20 uL total reaction volume. 0.16 uL forward primer, 0.16 uL reverse primer, 10 uL master mix (Nucleogene, Turkey) and 4.68 uL nuclease free water was used in each reaction for the genes SOX-2, Nanog and GAPDH. For the Oct-4 gene 5uL mixed forward and reverse primer solution (Nucleoge, Turkey), 4 uL cDNA, 10 uL master mix and 1uL nuclease free water was used. Reaction was performed in 45 cycles of quantification (95C°, 15s denaturation, 60C°, 30s annealing, 72 C°, 15 s elongation in each cycle) in thermocycler (Roche LightCycler 480 II, Sweden). GAPDH housekeeping gene used as a reference gene and gene expression analysis were performed by –ΔΔCT calculation. All calculations were performed in Excel. Graphs were plotted in GraphPad Prism 5.0.

3.6. Establisment of Cisplatin Resistant MDA MB 231 Cell Line

Cisplatin resistant MDA MB 231 cells were established by continuous exposure to Cisplatin (Cayman 13119, USA) of MDA MB 231 cells. Treatment concentration was calculated with MTT assay. Cells were seeded in t25 cell culture flasks and treated with IC20 (8.3 uM) cisplatin for 3 days. After 3 days, dead cells were removed by washing with PBS and cell media was changed with fresh media without cisplatin. Cells were kept in fresh media until they start to grow again. Afterwards fresh media was replaced with

media containing IC20 cisplatin. This cycle of cisplatin treatment was repeated for at least 3 times. At the end of treatment cycles, living cells were collected and their resistant phenotype was investigated. For all further experiments, cisplatin resistant MDA MB 231 cells were mantained in complete DMEM (5% FBS) media containing IC5 (3.56 uM) cisplatin at 37 C°, %5 CO_2 incubator (Nüve EC160, Turkey).

3.7. Viability (MTT) Assay

Cell viability assay was based on the ability of living cells to convert MTT (3-(4,5-dimethylthiazol-2-yl)-2,5-diphenyl tetrazolium bromide) reagent to formazan salts with the activity of mitochondrial enzyme succinate dehydrogenase (Fotakis and Timbrell 2006). Cells were seeded in 96 well plate with a confluency of 1×10^4 cells per well. After 24 hours of cell attachment, cell medium was removed, cells were washed with PBS and new media was added with escalated drug concentrations. For the cisplatin, the following concentration range was used: 1.56 uM, 3.13 uM, 62.5 uM, 12.5 uM, 25 uM and 50uM. After 3 days of treatment, cell media was removed, cells washed with PBS and new media with 0.25 MTT (Neofroxx 1334GR005, Germany) solution was added. After 4 hours of incubation at 37 C°, %5 CO_2 incubator (Nüve EC160, Turkey), media was removed and formed formazan salt was dissolved with 100 ul 1:1 ethanol/DMSO solution. 1:1 ethanol/ DMSO was used as a blank. Plate was put on a shaker (Heidolph Inkubator 1000, Germany) to totally dissolve formazan salt in wells followed by absorbance (Abs) reading at 570 nm in microplate reader (Tecan Infinite 200Pro). Cell viability was calculated after substracting the avarage of blank values according to the following formula below:

$$\%\ \text{Cell Viability} = \frac{(\text{Avarage Abs of treated cells})\times 100}{(\text{Avarage Abs of control cells})}$$

3.8. Doubling Time and Adjustments

Doubling time was calculated to study difference between resistance and sensitive phenotype of MDA MB 231 cells. To this end, 2.5×10^4 cells were seeded on 24 well plates in triplicates to be counted after day 0, day 1, day 2, and day 3. For counting, medium of each groups of cells was removed, cells were washed with PBS and detached by incubation with 50 ul of 0.25% Trpsin/EDTA solution (Gibco™ Catalog number: 25200056) for 3 minutes in 37 C° %5 CO_2 incubator. Detached cells were collected with 500 ul of cell media and counted. Same steps were performed for each follow up day. Doubling time was calculated with the formula below:

$$\text{Doubling time (hours)} = \frac{\ln(2) \times \text{incubation time (hours)}}{\ln \frac{\text{average number of cells at day x}}{\text{average number of cells at day 0}}}$$

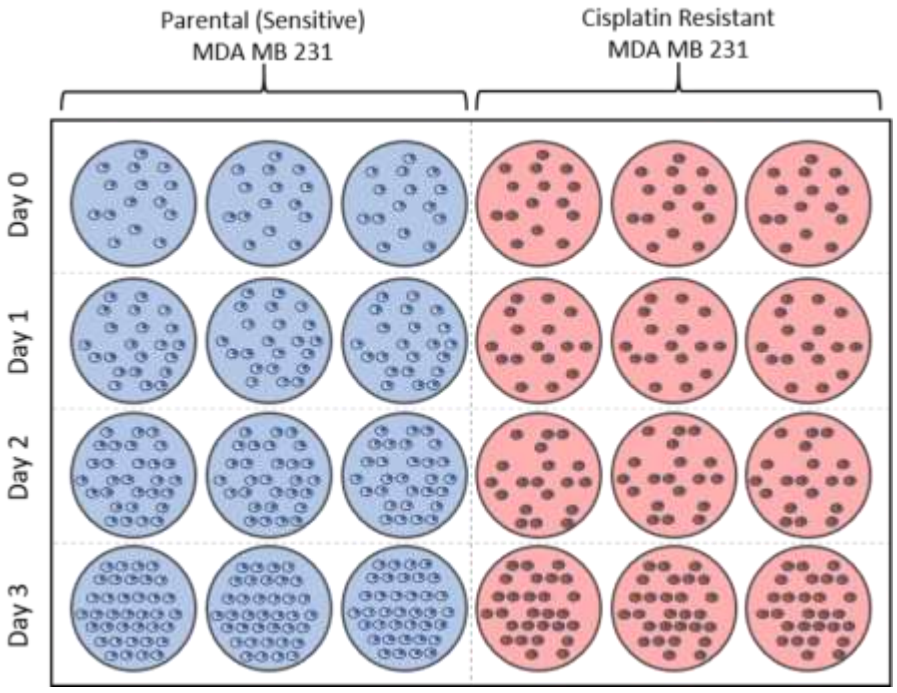

Figure 6. Representative scheme of doubling time analysis in a 24-well plate.

3.9. Colony Formation Assay

Colony formation assay was performed to make an inferration about dissemination and colony formation ability of resistant and sensitive cancer cells. For this assay, both cisplatin resistant and parental (sensitive) MDA MB 231 cells were seeded with the confluency of 2×10^3 cells per well in 6 well plate. After 24 hours of cell attachement, cells in two of the wells treated with IC5 cisplatin (3.56 mM) and cells in two of the wells was treated with IC15 cisplatin (6.86 mM) in both parental and resistant cells. After 3 days of treatment, cell media was changed with fresh media. Cells were incubated at 37 C°, %5 CO_2 incubator for 10 days. At the end of 10 day, cell media was removed, wells were washed with PBS and cells were fixed with cold methanol for 15 minutes at -20 C°. After fixation, cells were stained with 0.5% Crystal violet solution for 15 minutes. Stained cells were washed with PBS 3 times until there is no purple color comes off. Based on size (apx 50 cells per colony), the number of formed colonies were quantified.

3.10. Cell Migration (Wound Healing) Assay

Silicone inserts with a defined cell-free gap (Ibidi Culture-Insert 2 Well, Germany) were used for the formation of ‘’wounds’’ (gaps) in cell confluency. In the first place plastic inserts were sterilized in ethanol and dried under the hood. Then, inserts were places onto each well of 24 well plate by a tweezer. Parental (sensitive) and cisplatin resistant cells at the density of 2.5×10^5 cells per each insert chamber were seeded. After 5 hours of cell attachement inserts were removed from wells and the gap images were taken every several hours with inverted light microscope. Distance in the gap was measured with Image J (1.47T, USA) software.

3.11. Antibiotics Screening

Inhibitory activity of antibiotics from a drug library (Medchemexpress HY-LD-000003777, Sweden) on cisplatin resistant and parental (sensitive) MDA MB 231 cells were investigated with MTT assay. For each experiment at least 5 escalating concentrations of a drug were used in triplicates following frocedure described above in 3.2. After that, IC50 was determined following GraphPad Prizm 5.0 software. The actual IC50s were adjusted to the cell doubling time.

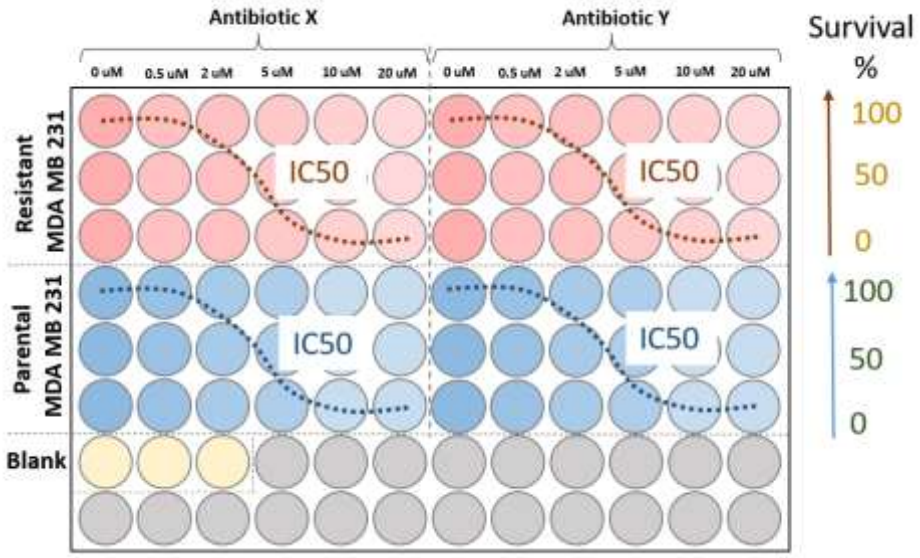

Figure 7. 96-well plate set up for screening antibiotics. In each plate two antibiotics were screened with 5 elevated concentrations.

3.12. Tumorsphere Assay

MDA-MB-231-based mammosphere from 3.2 were grown up to G3 in Poly-HEMA (Santa Cruz Biotechnology, Germany, sc-253284) coated T25 flasks followed spinning, dispergation on single cells in 0.5% trypsin/PBS solution and placing in Poly-HEMA coated 24 well plates in quadruplicates at a density of 500 cells per well. G3 cells were maintained in Cancer Stem Cell medium containing DMEM and bFGF/EGF mixture (10

nM final, each) with or without selected antibiotics taken at IC20 concentrations. 3 days after, images were taken under the light microscope at x20 objective (Zeiss) and the number of mammosphers of generation (G4) was counted followed by statistical analysis.

3.13. ATP Assay

ATP colorimetric assay kit (Elabscience E-BC-K157-M) was used to determine ATP level of cells. Parental and resistant MDA MB 231 cells were treated with 790 uM Amoxicillin sodium and 345 uM Fosmidomycin Sodium salt for 3 days. Non treated parental, resistant and cancer stem cells (CSC's) also grown for 3 days. After 3 days, cells were collected and counted. 2×10^5 cells were used for each group of cells. Cells were lysed in 100 uL RIPA buffer, sonicated for 2 minutes and centrifuged at 15.000 g for 10 minutes. 30 uL supernatant were used to test ATP content as indicated by insturactions of manufacturer.

3.14. Measurement of Mitochondiral Complex II activity

Complex II activity assay kit (Elabscience E-BC-K-150-M) was used to determine complex II activity. Parental and resistant MDA MB 231 cells were treated with 790 uM Amoxicillin sodium and 345 uM Fosmidomycin Sodium salt for 3 days. Non treated parental and resistant cells also used as a control. 1×10^6 cells collected as mentioned in Measurement of Mitochondiral Complex I activity part. Cells were mixed with reagent provided in the kit and centrifuged for 5 mintes. Supernatant was collected and centrifuged again at 15.000 g for 10 minutes. Precipitates were collected and mixed with other reagents provided in the kit and sonicated for 1 minutes. The mixture was centrifuged at 15.000 g again for 10 minutes. Supernatant was used to determine complex II activity as indicated by manufactureres' instructions.

3.15. Measurement of Oxygen Consumption Rate

Oxygen consumtion rate (OCR) of cells was measured via clark type oxymeter (Hansatech Oxygraph+, U.K). Chambers in which cells will be inserted were connected to 37 C° water bath to keep temperature stable inside the chambers during measurements. 4 drops of 50% KCl solution was dropped on top and sides of the electode. A thin piece of cigarette paper and an membrane which covers the electode disc put on top of electrode. Cigarette paper and membrane was fixed on electrode by a rubber disk. Electrode was connected to sensor device and waited until oxygen signal gets stabilized. Next, electrode was connected to chamber. 600 ul 37 C° PBS was inserted in the chamber and oxygen measurement started while stirring at 70 rpm with magnetic stirrer ability of the oxygraph. Oxygen level of PBS used as a blank and onset point. These steps were performed for two electrodes and two devices at the same time to measure oxygen consuption rate of two group of cells simulatenously. After oxygen consumption signal is stabilized, 5×10^6 of parental (sensitive) or cisplatin resistant MDA MB 231 cells dissolved in 600 ul of PBS were inserted in each individual chamber. Chambers were closed with screw pluggers, each having thin sealable hole for injection (Figure 7).

Change in the oxygen level of cell suspensions was measured for 5 minutes. Then, 20 uL of ADP (Sigma Aldrich, A2754) was added on cell suspensions as a substrate for mitochondrial respiration (OXPHOS) and oxygen level was recorded for 3 minutes. 20 uL of FCCP (Medchemexpress HY-100410, USA), an uncoupler of the proton gradient generated by the mitochondrial membrane, was added to cell suspensions and oxygen levels were recorded for 2 minutes. Lastly 20 uL of Rotenone (Medchemexpress HY-B1756 USA), an inhibitor of respiratory complex I, was added to cell suspensions to stop respiration. Cells were collected from chambers and stored in 70 uL RIPA buffer at -80 C° for protein profiling.

To measure OCR, two preselected in 3.6 antibiotics were used in almost all of the follow-up exeriments: Amoxicillin sodium salt (Amx) and Fosmidomycin sodium salt (FSS). Parental and resistant MDA MB 231 cells were treated with 790 uM of Amx and 345 uM FSS for 3 days and collected for OCR measurement.

OCR was calculated with the Oxytrace+ software designed by Hansatech (U.K.) The OCR/time graphs were plotted with GraphPad Prism 5.0.

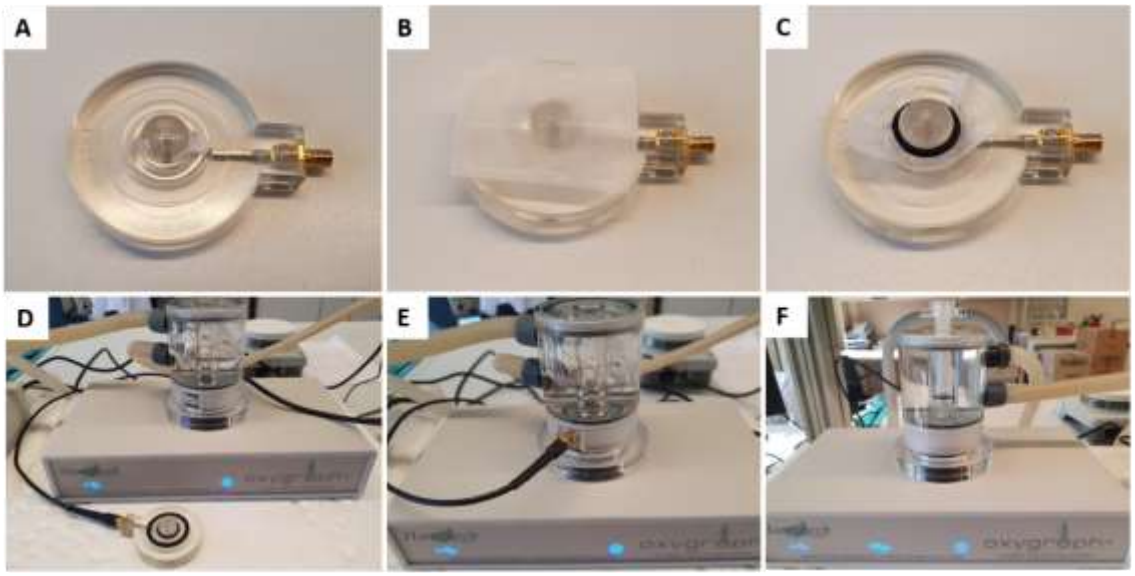

Figure 8. Components of Clark-type oxygraph and its assembly. A) a platinum electrode; B) a cigarette paper and a membrane was inserted on top of the electrode; C) paper and membrane are fixed to the electrode with a rubber; D) the electrode connected to device with a cable; E) the electrode conected to the chambers; F) cell solution is put to the chamber for measuring OCR.

3.15.1. Measurement of Oxygen Consumption Rate with XF24 Analyzer

OCR was also measured with Seahorse XF24 analyzer (Agilent Technologies, Spain). Parental and resistant cells (5×10^4 cell/well) were seeded in XFe 24-well plates (triplicates). Cells treated with IC20 concentration of Amx and FSS for three days. Upon three days of treatment cells were washed with PBS. Meanwhile, XF media (Agilent Technologies, USA) was prepared by supplementing with 2 mM L-glutamine, 2 mM pyruvate and 5.5 mM glucose. Suplemented XF media warmed and added to wells. Cells were incubated for 1 hour at 37 C°, CO_2-free incubator. Mitochondrial parameters were measured with Cell Mito Stress Test kit in XF24 Analyzer. Meanwhile protein concentration was measured with BCA assay (Pierce ThermoFisher 23227, USA) to make normalizations.

3.15.2. Isolation of Mitochondrial Subparticles

Mitochondial subparticles were isolated from 10.000 cells. Cells were collected and centrifuged at 600 g for 10 minutes. Cell pellet dissolved in cold buffer containing Tris–HCl (30mM), sucrose (75mM) and mannitol (225mM) and homogenized. Homogenized cells were centrifuged for 5 minutes at 600g at 4 C°. Pellets were dissolved in fresh buffer (Tris–HCl, sucrose and mannitol) and centrifuged at 7000 g for 10 min. After transferring supernanat to another tube, pellet was dissolved in buffer again and centrifuged at 10 000 g for 10 min. Supernanant was transerred and pellet was dissolved in buffer with HEPES (5mM pH 7.4), EGTA (0.5mM) and mannitol (250mM) and kept frozen at -80 C° in the presence of protease inhibitor (Kumari et al. 2014).

3.16. Mitochondrial Content Assay

Parental (sensitive) and cisplatin resistant MDA MB 231 cells were treated with 790 uM of Amx and 345uM of FSS for 3 days, collected and counted. Non treated Parental and Resistant cells were also collected and counted as controls. 2×10^4 cells from each group in triplicates were seeded on 96 well plate. After 1 hour of cell attachement, cell media was changed with 50 ul 1% MitoTracker (MitoGreen, Invitrogen™ M7514, USA) containing media. Cells were incubated at 37 C°, 5% CO_2 incubator for 25 minutes and the media was discarded, cells were washed two times with Penicillin/Streptomycin free media and 50 uL of PBS was added to each well. Fluorescence measurement at exitation length 485 nm and emission length 515 nm was performed on spectrophotometer (Molecular Devices, SpectraMax Gemini™ XPS/EM, UK). Results were statistically measured and plotted as bar diagrams.

3.17. Measurement of Metalloproteinase (MMP) Activity

MMP activity was measured with zymograpgh assay. 2.5×10^5 cells were seeded in 24 well plate wells. After 6 hours upon cellular attachment to the well surface, media of cells

were changed with FBS free media. Media of the cells which will be treated with selected antibiotics changed with the FBS free media having either Amx (790 uM) or FSS (345 uM). Polyacrylamide gel containing 0.1% gelatin was prepared. Samples from each media incubated with cells for 3 days were used for loading. 22 ul of each sample premixed with nonreducing sample buffer were loaded on the gel. 5 uL of protein ladder (3-color Prestained Protein Marker 10-190 kDa Cat#HY-K1011 Medchemexpress) was used in a separate lane as a weigh marker control. The gel was run at 40V for 20 minutes and then at 140V for the next 50 minutes (BIORAD Mini Protean Tetra System, USA). After completion, the gel was washed 4 times with washing buffer to remove SDS acess for 20 minutes with agitation on shaker (Stuart gyro-rocker SSL3) followed by incubation in the enzyme-activation buffer for 10 minutes at room temperature. The buffer was again replaced with fresh one and the gel with the buffer were left at 37 C° incubator (Memmert BE500, Germany) overnight. On the next day, gel was stained with staining Coomassie brilliant blue solution for 1 hour with slow agitaton (Stuart gyro-rocker SSL3, USA) followd by 2 times washing and destaining solution with slow agitation. Destaining solution was changed several times and fresh destaining solution added on gel until clear bands are observed. Gels were scanned and the band intencities measured with a ImageJ 1.47t (USA) software.

3.18. Polyacrylamide SDS Gel Electrophoresis (SDS PAGE)

For the SDS PAGE 10% running and 4% stacking polyacrilomide gels were prepared with 29:1 Acyrlamide/Bisacrylamide (A.B.T Laboratory Industry). Running gel poured to glass casette (BIORAD Mini Protean Tetra System, USA) was polymerized by adding 0.001% of ammonium persulphate (10%) solution. After settlement of running gel and removing access of matrix water, stacking gel was poured on top of running gel and combs were inserted to form the wells. In parallel, cell pellets for the Western blotting were lysed with 100 uL RIPA buffer and sonicated for 2 minutes on ice. 10 uL cell lysate was mixed with 10 uL of Laemmli loading buffer (5x). Samples were boiled at 95C°, for 5 minutes and centrifuged at 12000 g for 2 minutes. 10 uL from boiled cell samples was loaded to each well. 5 uL of protein ladder (Medchemexpress Cat#HY-K1011, USA) was

loaded in a separate lane. Gel was run at 40V for the first 20 minutes and at 100V for the next 50 minutes.

3.19. Western Blotting

For the Western blotting, SDS page gel with probes was rinsed with PBS from debris and incubated in blotting buffer for a few minutes (Stuart gyro-rocker SSL3, UK). Meanwhile, fiber pads and filterpapers (Watman) were moisturized with blotting buffer. Polyvinilfloride (PVDF, GVS 1214429) membrane was soaked in methanol for 5 seconds and placed into blotting buffer. Gel and PVDF membrane was inserted and compressed as a sandwitch betweed two filterpapers and two fiberpads with the help of gel holder. Gel holder was inserted to blotting chamber, filled with cold blotting buffer and gel was blotted at 100V for 1 hour at room temperature. After blotting, membrane was rinsed with PBS and blocked with 5% skimmed milk TPBS solution for 40 minutes with slow rotation at room temperature. Membrane was washed with TPBS (1% triton X in PBS) 3 times followed by incubation at 4 C° with rotation with 10 ml of primary antibody (b-actin antimous pAb, AFG Scientific, 1:1000 dilution with TPBS) overnight. Membrane was washed 3 times with TPBS and incubated with secondary antibody (mouse-HRP, AFG Scientific, 1:10000 dilution in TPBS) for 30 minutes. Membrane was washed 3 times in TPBS and after adding 1ml of ECLong solution (Genedirex SM801-0500). The membrane was imaged with BIORAD ChemiDoc Touch Imaging System (US).

3.20. Statistical Analysis

Excel 2016 (Microsoft, USA) and GrapghPad Prism 5.0 (USA) was used to calculate IC50 values and statistical analysis. ImageJ 1.47t (USA) software was used to measure wound distance in cell migration assay and band intensities in MMP assay. Oxytrace+ software (Hansatech, U.K.) was used for OCR analysis. TotalLab 2.0 (UK) was used to analyse western blot.

4. RESULTS

4.1. Finding Inhibiting Concentration (IC) Value of Cisplatin in MDA MB 231 Cells and Establishing Chemoresistant Cell Line.

In order to create cancer resistant cell line, IC50 value of cisplatin on MDA MB 231 TNBC cells was calculated by the survival (MTT) assay. Cells were treated with 6 increasing concentration of cisplatin (serial dilution of 0 uM, 1.56 uM, 3.12uM, 6.25uM, 12.5uM, 25uM and 50uM) for 3 days and cell viability was detemined as 100 %, 97%, 94%, 84%, 62%, 29% and 7% respectively (Figure 9). IC 50 value was calculated with GraphPad Prism 5.0 as 14.17 uM.

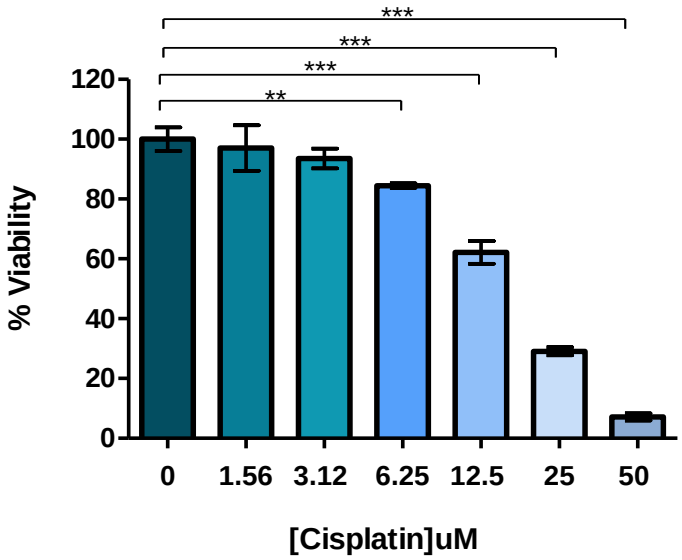

Figure 9. Cell viability assay. MDA MB 231 cells taken as triplicates were treated with increasing concentrations of cisplatin for 3 days and cell viability was determined by MTT assays. Experiments were repeated several times. * $P \leq 0.05$, ** $P \leq 0.01$, *** $P \leq 0.001$

Other calculated IC values indicated in the table below (Table 3) were used to mantain chemoresistant cells or for the tumosphere assays.

Table 3. Table that shows various IC concentrations for cisplatin on MDA MB 231 cells

IC50	**14.17 uM**
IC5	3.56 uM
IC10	5.34 uM
IC15	6.86 uM
IC20	8.29 uM
IC25	9.69 uM
IC30	11.11 uM
IC70	28.83 uM
IC80	37.28 uM
IC90	57.86 uM

To establish cancer cell line chemoresistant to cisplatin, sensitive MDA MB 231 cells were consequtively treated with 8.29 uM (IC20) cisplatin as described in method section and survived cells were collected and grown in no-drug containing complete DMEM. The procedure was repeated several times over 4-5 months, each time primary resistance was monitored by the MTT assay (Figure 10).

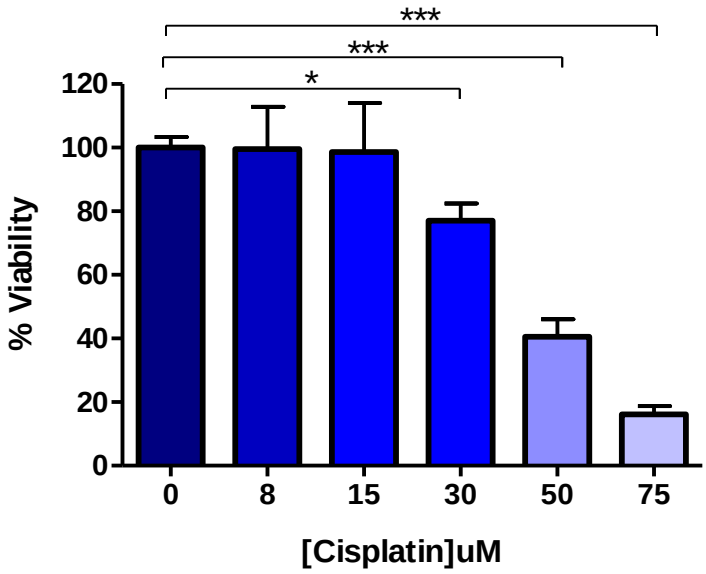

Figure 10. Acquired chemoresistance to cisplatin. MDA MB 231 cells undergoing interval treatment with predetermined IC20 concentrations of cisplatin for several months. Representative diagram of viability (MTT) assay shows chemoresistance aquisition. Experiments were repeated in triplicates several times. Error bars show standart deviation. P values for 0 vs 8uM and 0 vs 15uM was insignificant ($P \geq 0.05$). * $P \leq 0.05$, ** $P \leq 0.01$, *** $P \leq 0.001$

Treatment with increased concentration of cisplatin revealed a new IC 50 value calculated as 35.37 uM. This 3-time difference indicates aquired chemoresistance to cisplatin. After that, cells were multiplied, aliquoted and kept frozen at -80 C for further use.

4.2. Further Characterisation of Cisplatin Chemoresistant MDA MB 231 Cells

4.2.1. Cell Morphology and Doubling Time

To further characterize obtained cell lines, cells were studied for morphological differences. Interestingly, cisplatin resistant cells were bigger in size, which could be a result of multinucleation (Figure 11). Next, the doubling time was calculated by seeding same number of cells on 24 well plates for 4 time points (day 0, day1, day,2 day3). In

each day cells were collected and counted manually by hemocytometer with Trypan Blue dye and the doubling times were calculated as in Method section. The assay was repeated 4 times and 48 hours was selected for all further references as the most reliable time point for doubling time calculation. Doubling time of parental cells was determined as 28 hours while resistant cells had 53,8 hours of doubling time. This almost two times difference between cisplatin sensitive (parental) and resistant cells seems to indicate aquired mutations in the genes responsible for cell division.

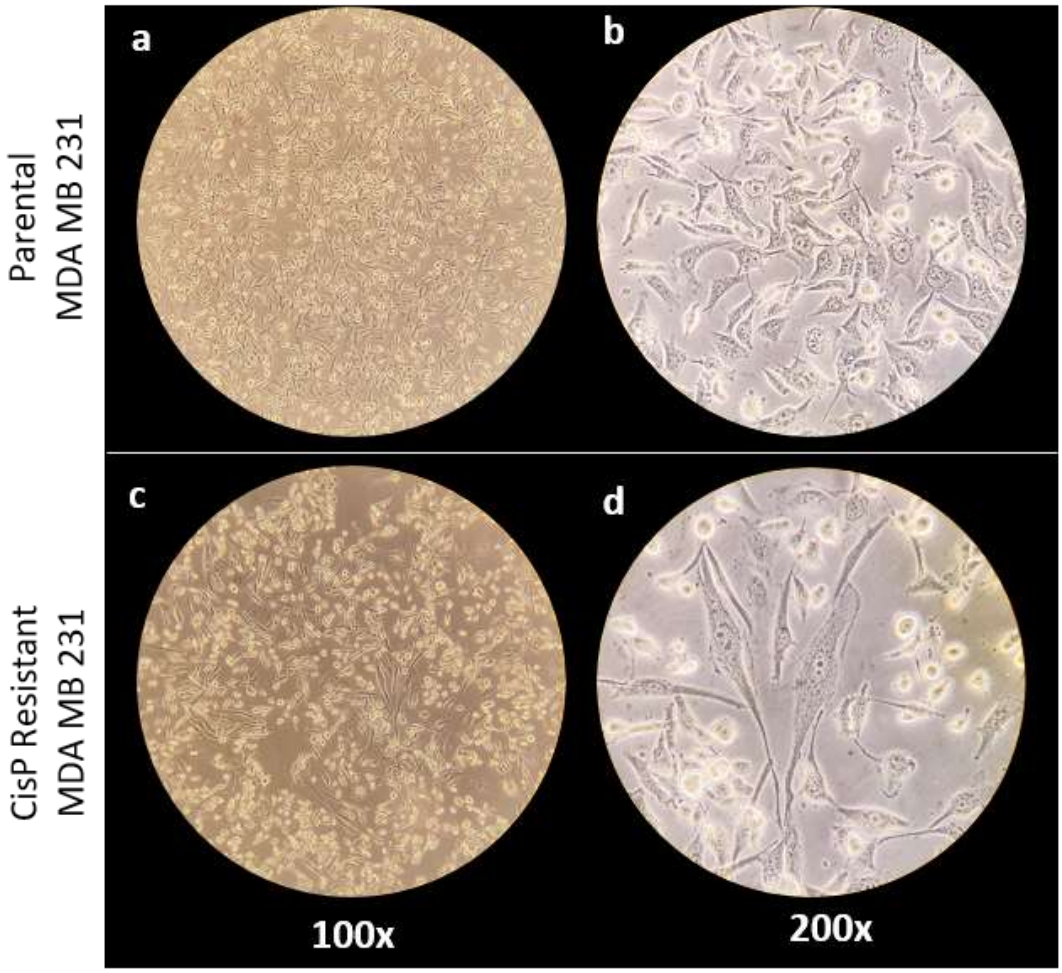

Figure 11. Morphologic differences between parental and cisplatin resistant MDA MB 231 cells. Parental cells are smaller in size and more homogeneal in shape compared to resistant cells. a) parental cells with 100x magnification b) parental cells with 200x magnification c) resistant cells with 100x magnification d) resistant cells with 200x magnification

4.2.2. Colony Formation Assay

Colony formation assay is used to understand the ability of cancer cells to dissiminate. The assay was performed both with parental and resistant cells seeded in 6 well plates with the 2000 cell/well and incubated for 10 days to form colonies, as indicated in the methods section. After 10 days cells were fixed with cold methanol and stained with crystal violet (Figure 12, A). The results give an example of an average number of colonies in parental cells (205) vs resistant counterparts (34) (Figure 12, A, a, d). Although resistant cells are normally having more metastatic capacity, such difference is likely to reflect the difference in the doubling time between parental and resistant cells during 10-day-experiment. However, after treatment with IC5 of cisplatin colony number significantly decreased (P=0.0129) to 28 in parental cells (Figure 12, A, b) while colony number almost did not altered (31 colonies) in resistant cells (Figure 10, A, e). After IC15 treatment, there was not any colony in parental cells (Figure 12, A, c) while resistant cells formed 14 colonies (Figure 12, A, f).

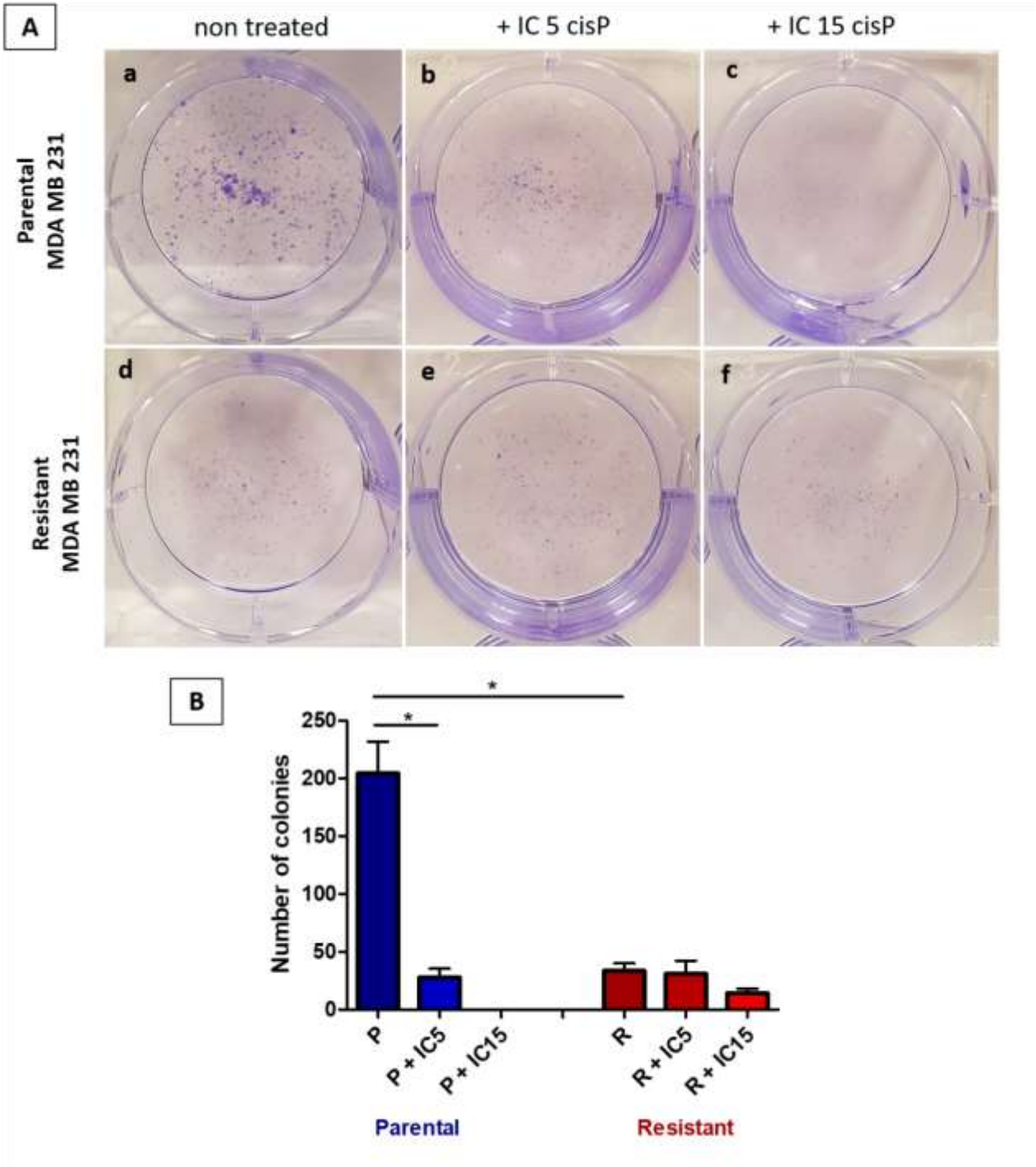

Figure 12. Colony formation assay. (A) MDA MB 231 cells seeded in 6-well plates at low density of 2000 cells per well were left in DMEM or treated with IC5 and IC15 cisplatin for 3 days, then allowed to grow for 10 days (n=2). Shown are example of stained parental (upper) and resistant (middle) cell images. (B) Bar diagram shows the average number of colonies after 10 day of incubation. Error bars represents standart deviation. * $P \leq 0.05$.

4.2.3. Migration of Cancer Cells

Migration of cancer cells serves as a universal indicator of malignancy and largely reflects their metastatic nature (Liu et al. 2020). For that reason, a wound healing assay was performed to compare spreading capacity of parental and resistant MDA MB 231 cells. Cells were placed into the inserts as indicated in methods, and were allowed to grow for the indicated time intervals followed by calculation of average gap filling after 0h ,7h, 19h and 24h, respectively (Figure 13). Images were taken and at each time point the distance was measured from 3 random sites. The most significant difference in migration was observed between parental (38.09%) and resistant (67.40%) cells at 24h. This 1.8 times difference indicates that resistant cells, despite having higher doubling time, migrate much faster than parental counterparts reflecting their metastatic potential.

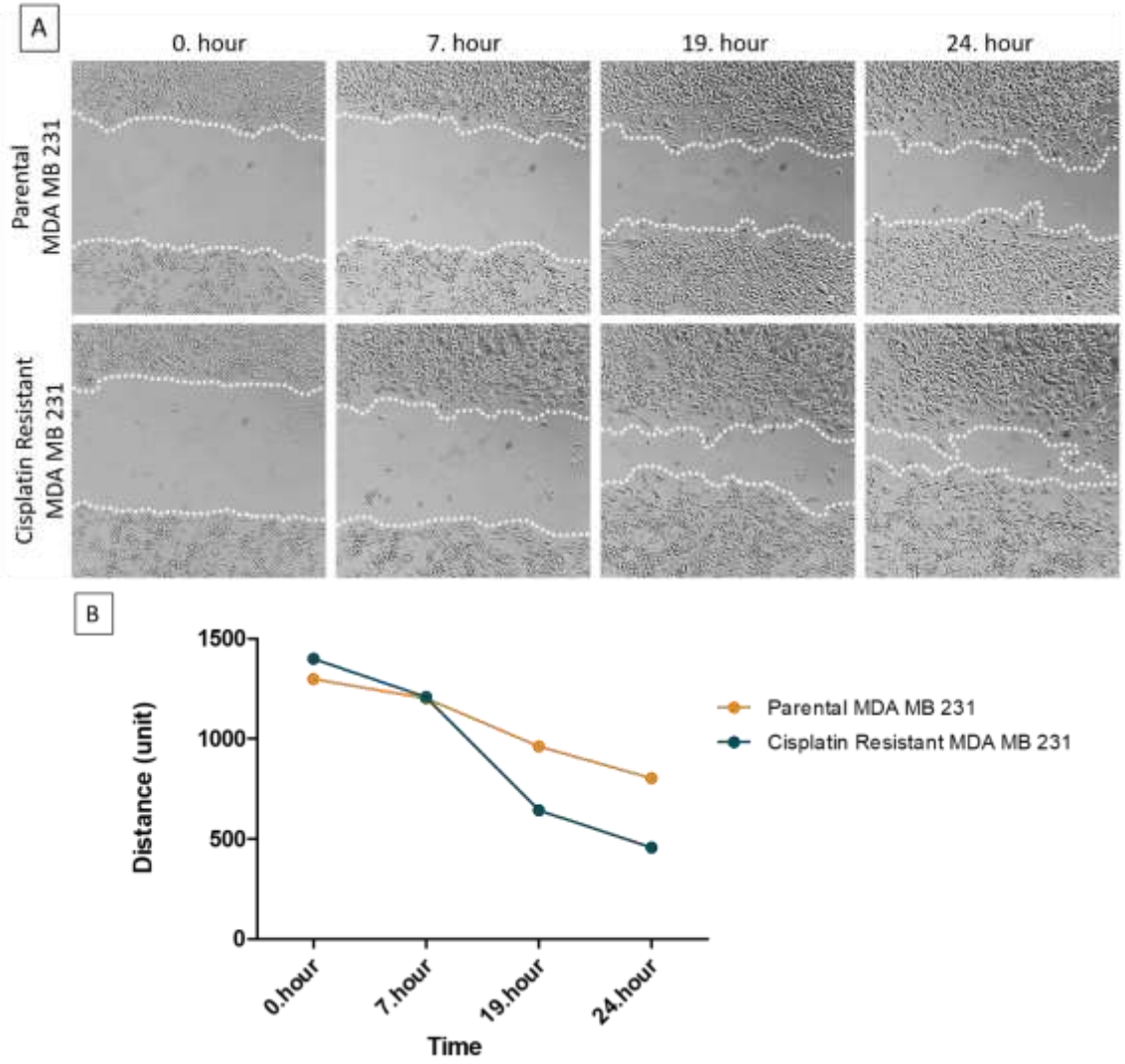

Figure 13.Wound Healing Assay (A) Representative example of images for parental (upper panel) and cisplatin resistant MDA MB 231 cells (middle panel) after removing wound forming inserts. Images were taken with Zeiss contrast-phase microscope (20x). (B) Representative example of time-dependent gap filling is shown on the graph (panel below) for parental (red) and resistant (blue) MDA MB 231 cells. All measurements were statistically significant.

4.2.4. Resistant and Sensitive MDA MB 231 Cancer Cells Reveal Difference in Respiration

Cellular respiration of eukaryotes is largely dependent on the mitochondrial function operating through the OXPHOS. In fact, 90% of oxygen uptake is thought to be hold by mitochondria. Our initial hypothesis states that heterogeneicity of malignant tumor may preserve resistant cells with more functional mitochondria, while sensitive cancer cells can be more prone for glycolysis or other means (Uslu et al, 2024). For that reason, obtained cell lines were tested for the OCR to identify possible differences. 5 million parental and resistant MDA MB 231 cells were used in 2-channel oxygraph to measure OCR. The highest OCR was 19.81 nA/m in parental cells and 56.05 nA/m in resistant cells as measured within the first 7 minutes. This may indicate that mitochondria-associated OXPHOS level was significantly higher in the cells with aquired chemoresistance. To test that, ADP (0.5 mM final) was injected to the oxygraph chambers. While the OCR was not altered significantly in parental cells with the highest rate of 26.51nA/m, in resistant cells OCR increased up to the value of 106.2 nA/m. These results suggest that cisplatin chemoresistant cancer cells are more OXPHOS dependent than their sensitive counterparts. Furthermore, adding uncouler FCCP (3.34uM final) did not reveal any significant OCR change in parental cells (30.9 nA/m) but was increased almost 7 times in the corresponding samples of cisplatin resistant cells (209 nA/m) (Figure 12). These effects indicate the contribution of mitochondria as adding rotenone (3.34uM final), respiratory complex I inhibitor, immediately decreased OCR in both parental and resistant cells.

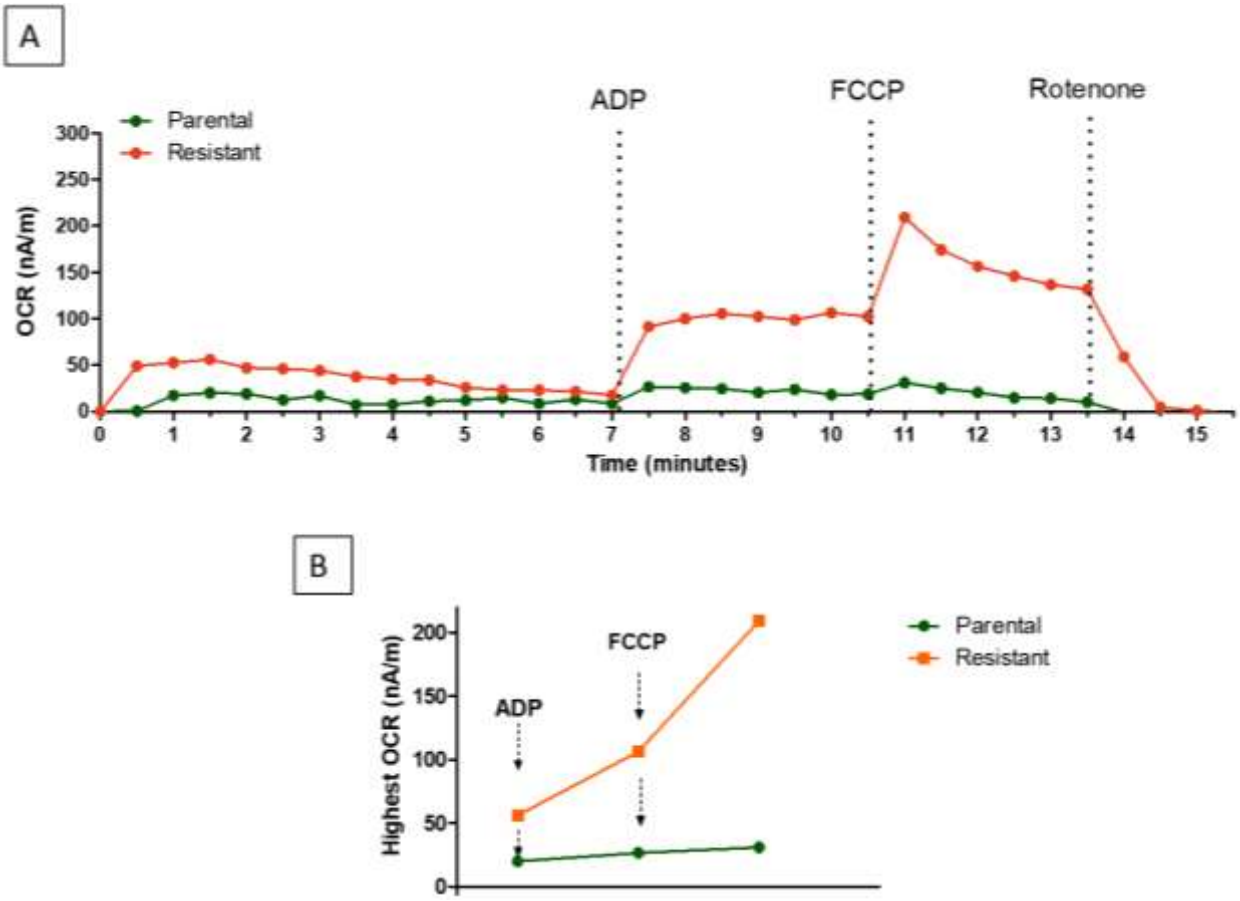

Figure 14. Oxygen consumption rate (OCR) of parental and resistant cancer cells. (A) Representative example of OCR profile of MDA MB 231 parental (green) and resistant to cisplatin (red) cells. 5 mln cells were placed into each chamber of the oxygraph and OCR was recorded. 7 minutes after, ADP (0.5mM) was injected into each chamber to stimulate OXPHOS. After 10.5. minutes, FCCP (3.34uM) was added and after 13.5 minutes, rotenone (3.34 uM) was injected. (B) Change in the highest OCR level after addition of ADP and FCCP in parental and resistant cells.

Since resistant and sensitive phenotypes of cancer cells reveal difference in OXPHOS dependence, OXPHOS inhibition can serve as a mean to specifically discriminate between two types of cancer cells. For that reason, drug repurposing approach was undertaken using a chemical library of over half a thousands of antibiotics. 59 Antibiotics from the library was selected to be secreened against parental and cisplatin resistant MDA MB 231 cells with MTT assay. Only the deugs which has broad range of activity or have an activity against gram negative (Gr-) bacteria were selected for screening. This is due to the aim of inhibition of resistant cells by targeting their mitochondira originated from

Gr- bacteria some billions years ago. Ratios of IC50s for antibioitics were calculated for parental and resistant MDA MB 231 cell via MTT assay and 4 antibiotics with the highest values (leads) were chosen as having higher toxicity for resistant vs. parental cells (Table 4). These 4 leads (Table 4, highlighted in brown-red) are amoxicillin sodium (Amx, IC50 ratio 2.66), fosmidomycin sodium salt (FSS, IC50 ratio 2.17), telithromycin (IC50 ratio 2.17), and oligomycin A (IC50 ratio 2.63).

Tablo 4. IC50 values of prescreened antibioitics from the drug library for parental and resistant MDA MB 231 cells with the ratios difference. 4 leads with lower inhibitory concentration for resistant vs parental cells are highlighted in red.

	Antibiotics	IC 50 for Parental cells	IC 50 for Resistant cells	Ratio of IC50's
1	Sulfathiazole	14,66	11,91	1,23
2	Chlorhexidine	8,70	8,73	1,00
3	8-Hydroxyquinoline	5,01	6,47	0,77
4	Tilmicosin	15,81	11,97	1,32
5	Amoxicillin (sodium)	210,21	78,99	**2,66**
6	Fosmidomycin sodium salt	173,92	80,06	**2,17**
7	Tildipirosin	12,63	10,87	1,16
8	Tulathromycin A	13,17	10,51	1,25
9	Nifursol	15,29	11,36	1,35
10	Sulfadimetoxine	17,50	12,46	1,40
11	Cefmetazole	13,63	10,46	1,30
12	Quinocetone	8,57	7,80	1,10
13	AFN 1252	11,33	7,30	1,55
14	Lexythromycin	13,63	8,07	1,69
15	Betamipron	14,90	8,76	1,70
16	6AON	14,09	10,86	1,30
17	Cefazedone	13,83	6,72	2,06
18	Cefdinir	14,56	7,07	2,06
19	Clioquinol	8,74	5,93	1,47
20	Ceftocalin fosamil	14,12	9,17	1,54
21	Ciprofloxacin	13,32	7,76	1,72
22	Plurifloxacin	10,93	5,90	1,85
23	Rotxythromycin	13,19	9,59	1,38
24	Sulfacetamide	12,93	9,94	1,30
25	Brilacidin	14,54	10,33	1,41
26	Sulfadiazine	13,66	6,71	2,03
27	Cefepime	11,16	7,30	1,53
28	Sulfadoxine	14,35	9,38	1,53
29	Nadilofloxacin	13,82	10,13	1,36
30	Telithromycin	12,93	5,97	**2,17**

	Antibiotics	IC 50 for Parental cells	IC 50 for Resistant cells	Ratio of IC50's
31	Trimethoprim	12,52	8,01	1,56
32	Cephapirin	12,94	10,90	1,19
33	Tylvalosin	7,63	4,38	1,74
34	CHIR 90	13,12	9,50	1,38
35	BRD 8000.3	14,98	13,91	1,08
36	Valvivudine	12,80	9,80	1,31
37	RNPA 100	14,48	11,10	1,30
38	Olygomicin A	10,87	4,14	**2,63**
39	Allicin	99,86	99,74	1,00
40	Ofloxacin	14,96	12,87	1,16
41	Moxalactane	15,67	13,64	1,15
42	Lefamulin	12,16	10,62	1,15
43	Apropitant	28,96	24,42	1,19
44	Clindamycin	14,12	9,32	1,52
45	Bacampicillin	12,82	9,98	1,28
46	Mycophenolic acid	3,69	3,42	1,08
47	Sibofimloc	12,53	6,17	2,03
48	Sulopenem	11,23	10,10	1,11
49	Ribavirin	10,07	7,33	1,37
50	Ampicillin	10,26	8,82	1,16
51	Difloxacin	9,44	11,74	0,80
52	Tebipenem	12,52	13,89	0,90
53	Rifabutin	9,09	9,79	0,93
54	Pipemidic Acid	9,74	11,50	0,85
55	Chlorquinaldol	6,13	7,14	0,86
56	Phloracephotenone	11,63	10,28	1,13
57	Cefuroxime	11,04	8,46	1,30
58	Nifuroxazide	8,44	9,63	0,88
59	Sulfachloropyrzadine	11,24	9,49	1,18

Olygomycin A was excluded from further studied despite having second highest IC50 ratio among 4 antibiotics. This is because oligomycin A is an ATPase inhibitor which anticancer activity was already well documented. From the remaining 3 leads, Amx and FSS were shortlisted to be further tested in biophysical and biochemical assays. Examples of IC50 difference for these drugs are shown in Table 4.

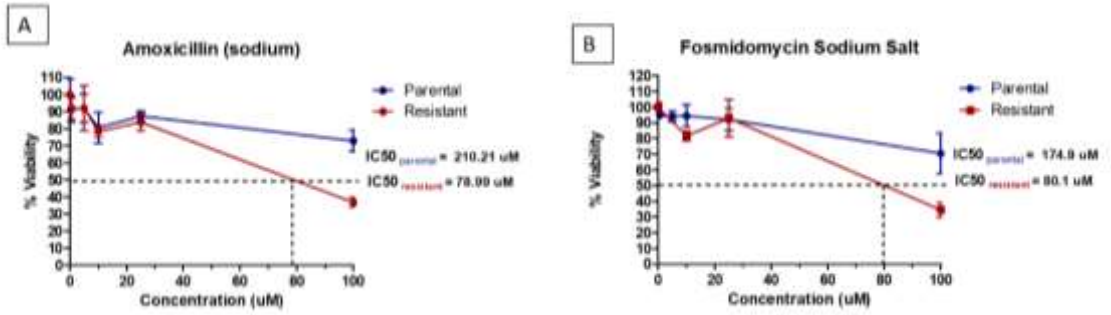

Figure 15. Amoxicillin (Amx) and fosmidomycin (FSS) can disciminate parental and resistant cancer cells. MDA MB 231 parental (blue) and resistant cancer cells (red) were treated with shortleasted antibiotics and MTT assayed after 3 days. IC50s were calculated accordingy. The assay was repeated in quadruplicates for several times and revealed significant difference

For a full scale experiments, new batches of Amx (Medchemexpress, HY-B0467) and FSS (Medchemexpress, HY-112853) were re-ordered separately from the drug library and their inhibitory concentrations were determined again with MTT assay as being 1021.44 uM (Amx) and 790.7uM (FSS) for paretal and 596 uM (Amx) and 345 uM (FSS) for resistant cells, respectively. The discrepency between old and new IC50 values was liklely linked to a batch to batch purity difference.

4.3. Testing Activities of Amx and FSS

4.3.1. Bioenergetic Demand

Cancer cells can produce ATP either with glycolysis or through mitochondrial OXPHOS. Previously known as Warburg effect, there are still contradictory evidence showing that some malignant tumors switch from OXPHOS to glycolysis to produce less ATP but in a fast manner. Our hypothesis is that within the same malignant tumor some slowly dividing CRC or CSCs rely on OXPHOS while majority of sensitive (parental) cancer cells undergo glycolysis (Uslu et al., 2024). In turn, antibiotics may suppres mitochondrial functions therefore decreasing OXPHOS and ATP production. In order to understand

whether antibiotics have a positive or negative effect on cellular ATP production, ATP level of parental, resistant, Amx and FSS treated counterparts and MDA MB 231 cancer stem cells was measured. Even with the lower number of cells, ATP level of CSC was significanly higher than in parental or CRC. Negative value of ATP level in parental cells represents a very low amount of ATP level close to the kit detection level. Accordingly, CRC have higher ATP level than parental and resistant cells. After Amx and FSS treatment ATP level increased to 14.4 M and 33.5 M respectively in parental cells ATP level increased 46% after Amx treatment while it decreased 72% after FSS treatment in resistant cells (Figure 16).

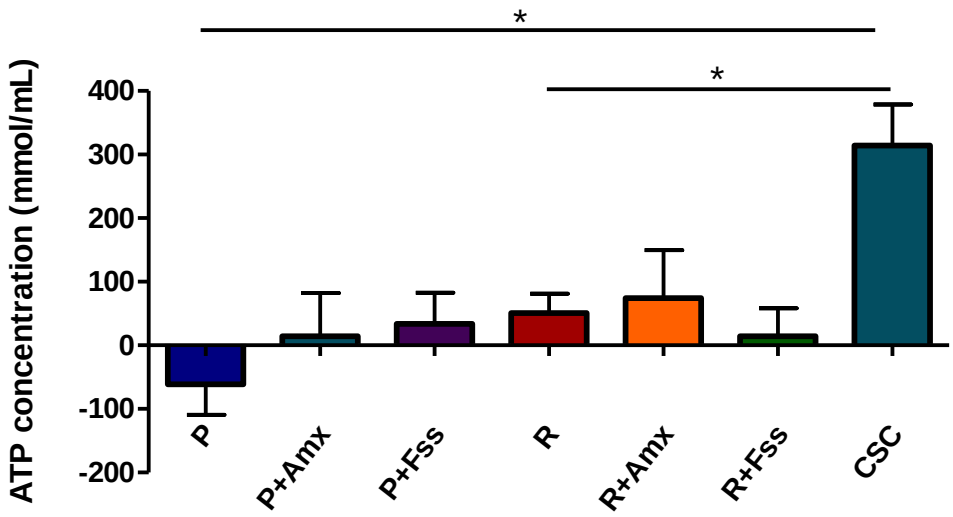

Figure 16. High levels of ATP in CSCs and CRC. Triplicates of MDA MB 231 parental (P), cisplatin resistant (R), and stem-like cancer cells (CSC) untreated or treated with 790uM Amx or 345 uM FSS antibiotics for 3 days followed by ATP spectrophotometric assay. Results were plotted as a diagram, where error bars represent standart deviation. * $P \leq 0.05$

4.3.2. Mitochondrial Complex II Assay

Since ATP increase in CRC vs. Parental cancer cells may be related to enhanced OXPHOS level, we studied activity of mitochondrial respiratory complexes. In a parallel study with MDA MB 468 cells chemoresistant too cyclophosphamide, complex II (CII)

was shown to have the highest activity among other complexes. Measurement of CII activity revealed 2.5 times higher activity for CRC vs parental cancer cells (Figure 17). Next, we tried to test whether treatment with selected antibiotics could decrease CII activity. For that part, CRC and parental cancer cells were treated with either Amx or FSS. To our surprize, treatment with Amx and FSS increased both parental (1.9 and 2.3 times, respectively) and resistant (0.08 and 0.36 times, respectively) activity of CII as shown on Figure 17.

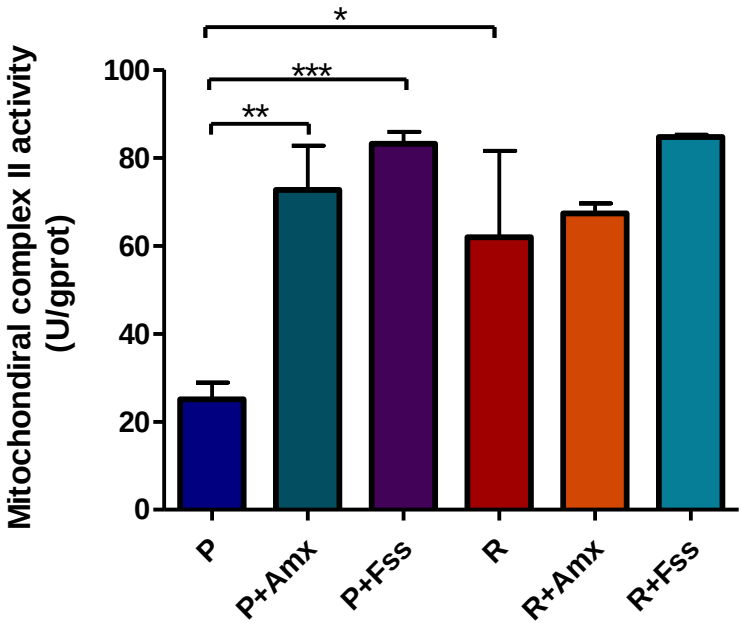

Figure 17. Mitochondrial complex II activity is higher in CRC compared to parental cancer cells. Triplicates of MDA MB 213 cisplatin resistant (R) or parental (P) cells untreated or treated with 790uM Amx or 345uM FSS for 3 days were assayed for CII activity and results were plotted on the diagram. Error bars represent standart deviation. * $P \leq 0.05$, ** $P \leq 0.01$, *** $P \leq 0.001$

4.3.3. Mitochondrial Content Assay

In order to explain partial increase in CII activities upon treatment of cancer cells with antibiotics, we performed mitochondrial content test to obtain an idea about the relative amount of mitochondria in the studied cells. This assay was performed by using

fluorescence mitochondrial dye Mitotracker™ Green. Relative fluorecsence intensities show that CRC have 2.1 times higher mitochondiral content than parental cancer cells (p= 0.01). Although statistically insignificant, after Amx (p=0.58) and FSS treatment (p=0.096), mitochondrial content increased both in parental (0.13 times in Amx and FSS, respectively) and resistant cells (0.07 and 0.22 times in Amx and FSS, respectively) (Figure 18).

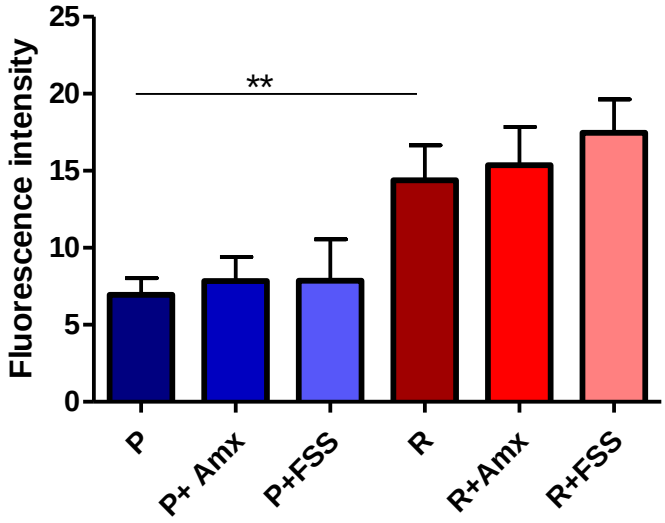

Figure 18. Increase in mitochondrial content upon treatment with antibiotics. Triplicates of MDA MB 231 cisplatin resistant (R) or parental (P) cells untreated or treated with Amx or FSS for 3 days were assayed for mitochondrial content using MitoGreen fluorescent assay. Relative intencities are shown on the diagram. Error bars represent standart deviation. ** $P \leq 0.01$

4.3.4. Oxygen Uptake Upon Treatment with Antibiotics

Difference in the OCR between CRC and parental cancer cells was already demonstrated in the 4.2.5 section. In order to investigate possible effects of Amx and FSS on cellular respiration and OXPHOS, OCR was measured using oxygraph device. Interestingly, Amx and FSS treatment increased OCR in both parental and resistant cells without stimulating OXPHOS suggesting mitochondria-independent oxidative activity. Highest OCR was 71.7 nA/m in parental cells and 81.8nA/m in parental cells treated with Amx (P+Amx),

and 91.5 nA/m in parental cells treated with FSS (P+FSS) first 5 minutes. After promoting OXPHOS by adding ADP, OCR did not significantly change in parental cells (Figure 19, A) treated with Amx and FSSbut did change in resistant cells (Figure 19, B). After adding uncoupler FCCP, OCR continued to decrease in parental cells and was increased up to 178.2 nA/m in the Amx pretreated cells. An abrubt increase was not observed in parental cells treated with FSS cells. In resistant cells, the highest OCR was 65 nA/m and reached 80.9 nA/m and 109.1 nA/m in the CRC treated with Amx and FSS, respectively.. After FCCP injection, OCR inclined to 141.3 nA/m in resistant cells, 207.8 nA/m in Amx treated cells and 188.7nA/m in FSS cells cells (Figure 19, B).

A

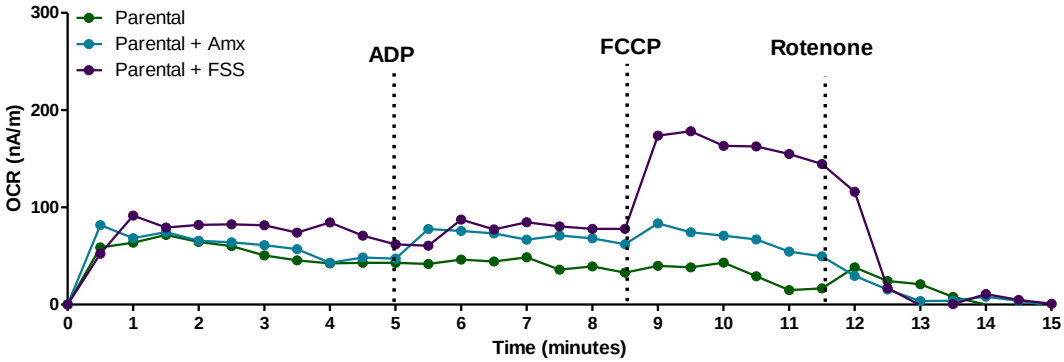

B

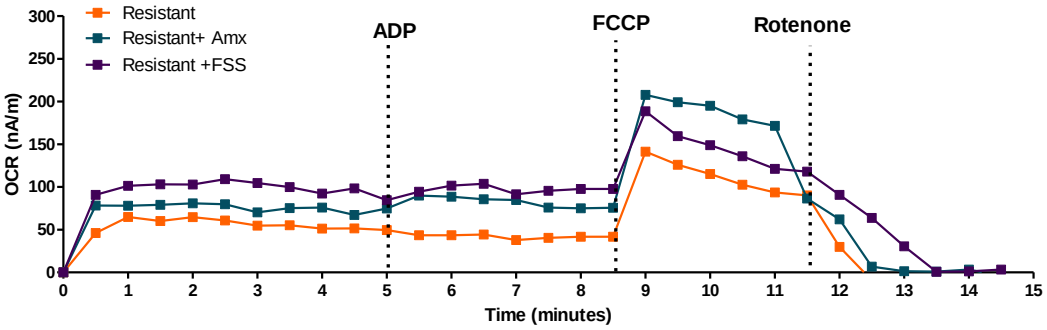

Figure 19. OCR study in resistant and parental cancer cells upon treatment with antibiotics. Parental (A) or resistant (B) MDA MB 231 cells were untreated or treated with antibiotics Amx (790uM) or FSS (345Mm) followed by OCR measurement in multichannel oxygraph. ADP (0.5mM) was added ater 5 minutes and after 8.5. minutes FCCP (3.34uM) was added. 11.5 minutes after. rotenone (3.34 uM) was injected to cell solutions.

Overall, these result show that also OXPHOS level is high in cancer resistant cells, treatment with antibiotics also increase oxygen uptake independent on mitochondria.

To test this, we isolated mitochondrial subparticles from the parental and resistant cells and performed OCR measurements using SeaHorse apparatus (Figure 20). As shown below, both Amx and FSS suppressed OCR in mitochondria and adding ADP did not significantly stimulate cellular respiration suggesting that OXPHOS was also suppressed.

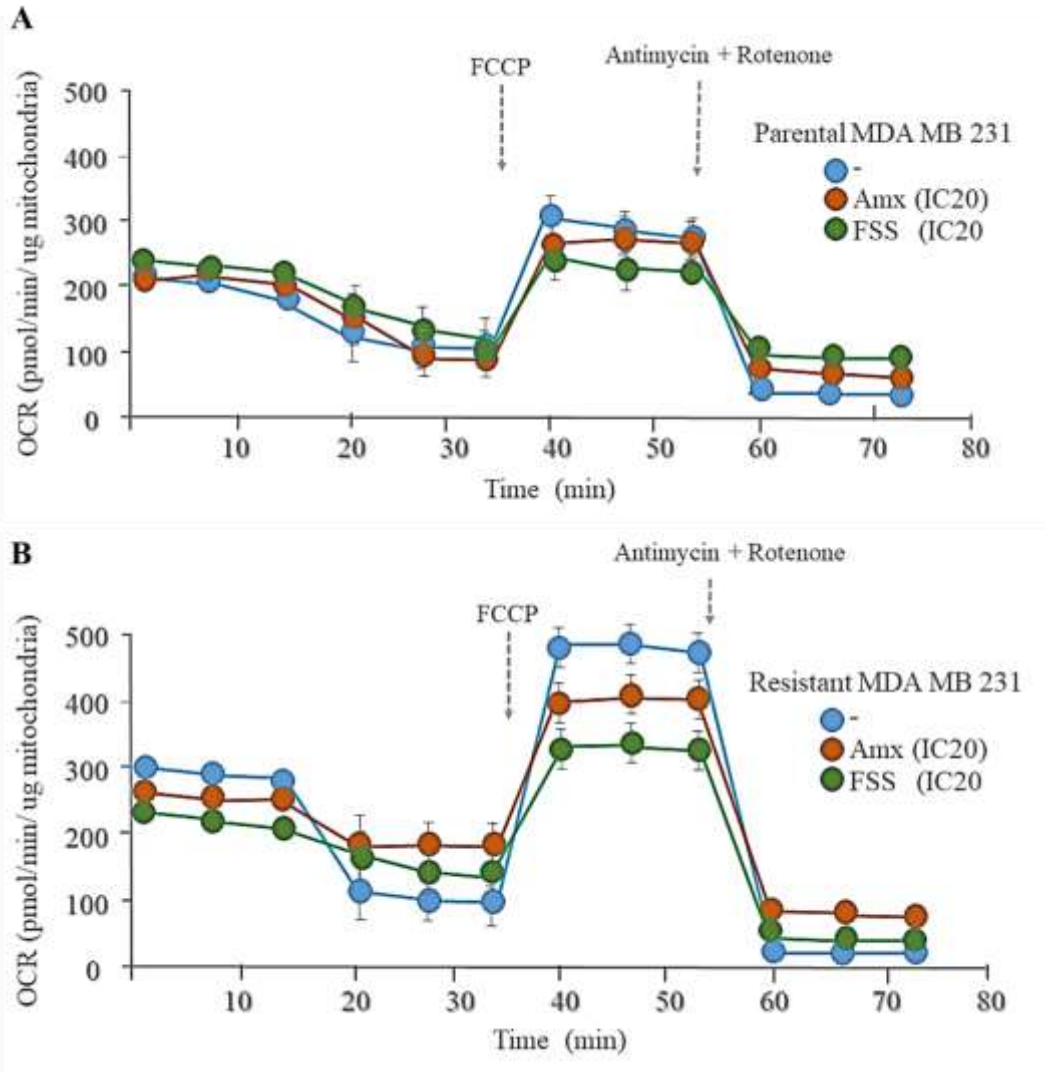

Figure 20. Seahorse analysis of OXPHOS in MDA MB 231 mitochondrial particles. OCR normalized to mitochondrial content in MDA MB 231 parental (A) and cisplatin resistant (B) mitochondrial subparticles incubated 30 minutes prior experiment in XF assay medium supplemented with 5 mM glucose and 2 mM glutamine and consecutively injected with ADP (10 μM), FCCP (1.5 μM), antimycin (1 μM) and rotenone (1 μM). Continuous OCR values (pmoles/min/μg mitochondrial proteins) are shown. Mean ± SEM (n=4). $p < 0.05$ for all experiments.

Alltogether, our finding revealed that antibiotics showing presumable anticancer activity against chemoresistant breast cancer cells may act by suppressing higher OXPHOS in these cells and did not significantly affect OXPHOS in sensitive (parental) counterparts. Additionally, the same antibiotics may promote oxygen uptake independently on mitochondria, most likely through microsomel/peroxisomal systems.

4.4. Testing Pathways Activated in Resistant and Parental Cancer Cells Upon Treatment with Antibiotics

Suppression of mitochondria-mediated OXPHOS by antibiotics may induce several pathways, starting from the mitochondria biogenesis and going to the apoptosis. To understand these pathways, protein profiling should be accomplished based on the OMICs data (ongoing research) and published literature. Here, I focused on testing several pathways that migt be involved in the switch from sensitive to parental cancer phenotype and at the same time, - tried to understand how selected antibiotics migh affect those pathways.

4.4.1. Measurement of Metalloproteinase (MMP) Activity

One of the reasons cancer cells become more agressive is through their ability to leave the original tumor site by developing specific traits. This often occurs through the activation of matrix metalloproteinases (MMPs), a group of endopeptidases playing a role in degradation of extracellular matrix proteins (ECM). ECM represent a physical barrier which has to be digested for cell invasion and metatasis (Kleiner and Stetler-Stevenson 1999). Increased activity of MMPs was correlated with metastatic ability of many tumors (Fukushima et al. 2018). To better understand the difference between parental and resistant cancer cells and study possible effects of Amx and FSS towards metastasis, MMP-2 and MMP-9 activity was investigated with gelatin zymograpgh assay. MMP-2 (gelatinase A) and MMP-9 (gelatinase B) can degrade variety of ECM proteins however,

their efficiency is higher for gelatin (Murphy and Crabbe 1995). Degraded bands on gelatin within an acrylamide gel provides a universal instrument to study MMP activities. MMPs are expressed in inactive form (pro MMPs) and become active after cleavage of their corresponding pro-domain (Page-McCaw, Ewald, and Werb 2007). For that reason, MMP 2 exists as 72 kDa inactive and 64 kDa active forms (Arps et al. 2013), while MMP-9 has 92kDa and 82 kDa forms, respectively (Christensen and Shastri 2015; Van Wart and Birkedal-Hansen 1990). To this end, cells assayed for the MMPs revealed several activities as shown on the zymogram below (Figure 21). MMP-2 bands intensity was almost equal in parental and resistant cells, even after treatment with Amx and FSS. However, pro-MMP-9 activity was higher in resistant cells (1.5 times) compared to parental cells. After treatment with Amx and FSS intensity of pro-MMP-9 band decreased (35% and 7.7%) in parental and resistant cells (33% and 30% respectively).

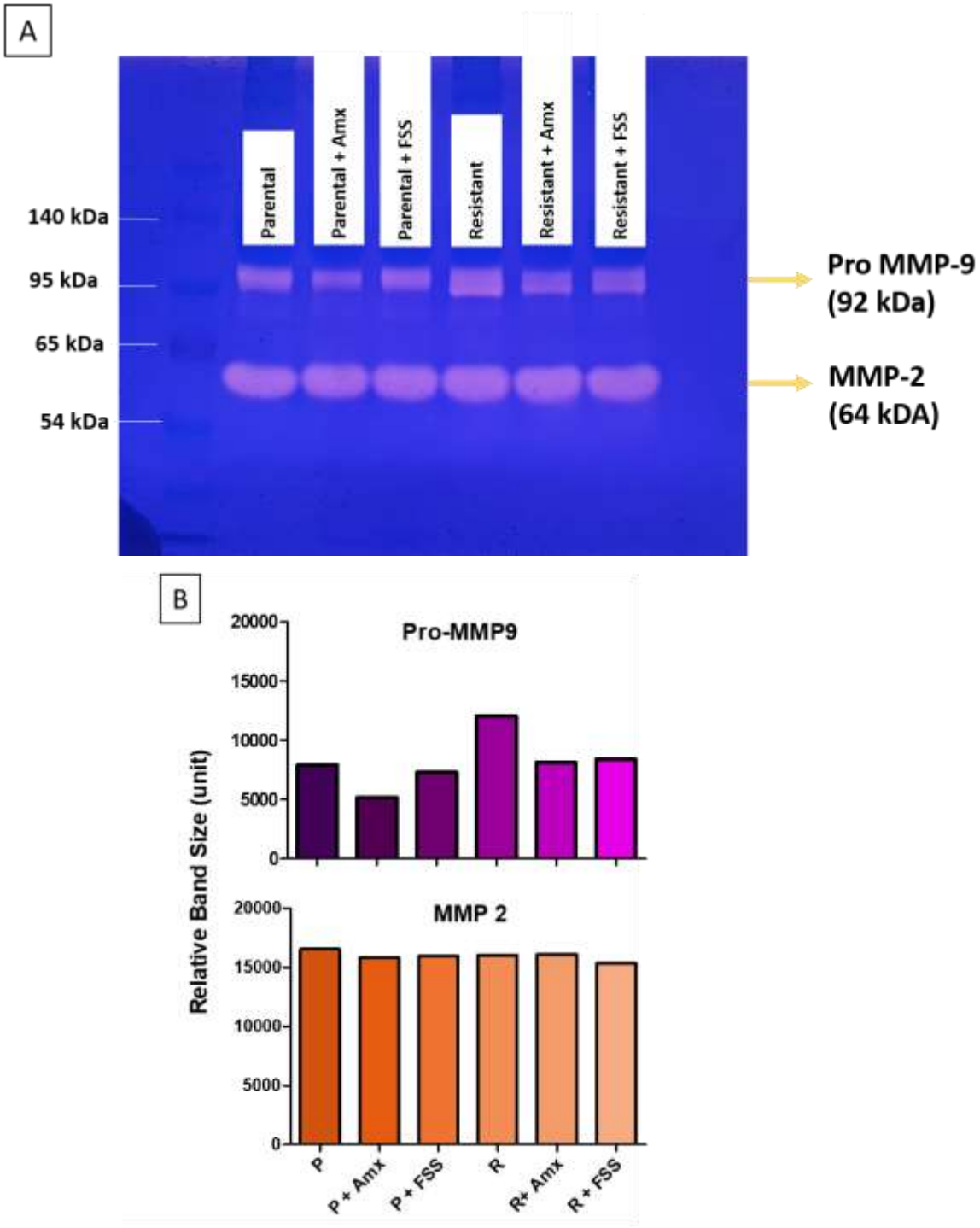

Figure 21. Gelatin zymography analysis. (A) MDA MB 231 parental (P) or cisplatin resistant (R) cells were untreated or treated with Amx or FSS antibiotics for 2 day and supernatants of media were assayed in 1% gelatin-10% polyacrylamide gel followed by incumation with MMP buffer to activate gelatin digestion. (B) Images of zymograph were digitized and signals from clear band areas representing MMP activities were plotted on the diagram.

4.4.2. Studying Stemness Genes by Real Time Quantitavie PCR

Cancer stem cells (CSC) and cancer resistant cells (CRC) share common characteristics like having resistance to chemotherapy and taking active role in metastasis. Since CSC have resistance to chemotherapy, CRC may demonstrate stemness properties. SOX-2 (Sex determining region Y box-2) and Nanog are two transcription factors playing a role in stem cell maintenance (Chambers et al. 2003; Schaefer and Lengerke 2020). In fact overexpression of *SOX-2* and *Nanog* is correlated with carcinogenesis and these two genes are known as oncogenes (Jeter et al. 2015; Lu et al. 2010). In this work, we created generation of cancer stem-like cells (CSCs) by growing parental cells in nonadhesive conditions with the media stimulated by bFGF, EGF and B supplement. Cells were allowed to form spheres known as spheroids or mammospheres. It is believed that in such forms they mimic a specific subset of cancer stem cells that are more agressive and more metastatic than corresponding parental counterparts. At the same time, CSCs may have similar qualities as resistant cancer cells (Abad et al, 2019). RT qPCR data revealed that resistant cells have 25% higher expression of *SOX-2* and 8.4% higher expression of *Nanog* as compared to the corresponding parental cells (Figure 22). Moreover, treatment with Amx antibiotic decreased the expression level of *SOX2* both in resistant (30%) and parental cells (24%). Similarly, this decrease was also obtained for *Nanog* (84% in resistant cells, 30% in parental cells). However, FSS treated samples revealed increased *SOX-2* and *Nanog* expression levels (35% and 15%, respectively) in parental cells while their resistant cells demonstrated 44% and 58% inhibition, respectively.

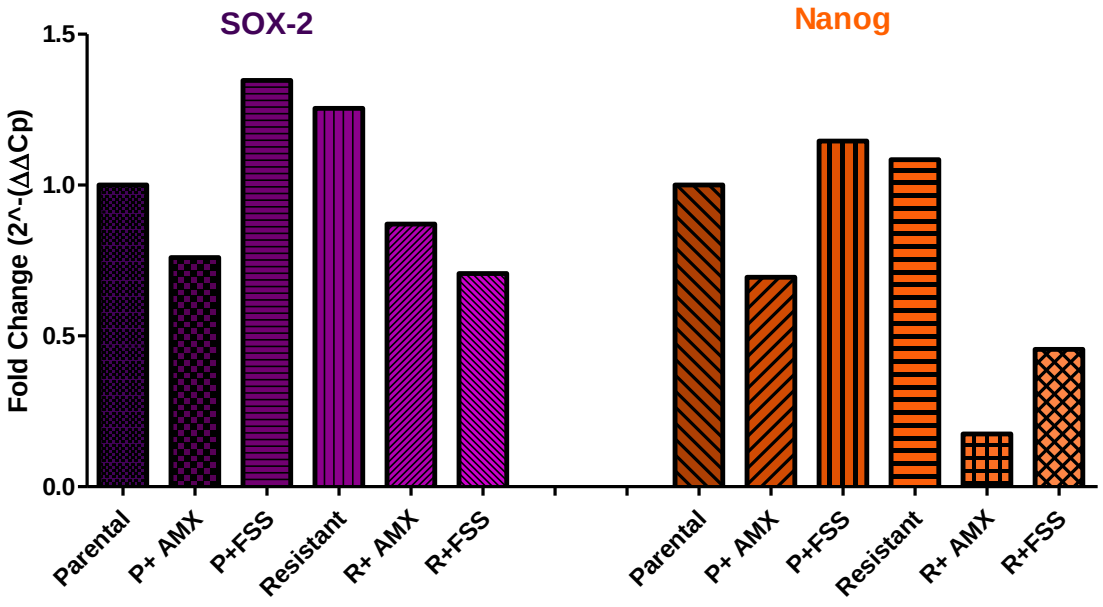

Figure 22. Antibiotics affect expression of stemness genes in cancer cells. Parental (P) or cisplatin resistant (R) MDA MB 231 cellstreated with either Amx or FSS antibiotics were processed for the RT-qPCR analysis with the primers corresponding to SOX-2 and Nanog. After normalization for GAPDH expression level, data were plotted on the pgraph as fold change differences. Experiments were done in triplicates. Data rerveal statistical significance.

4.4.3. Formation of Mammospheres

CSC forms colonies (tumorsphers or for the breast cancer – mammospheres) in non adherant conditions. These clones are observed with a spherical shape of ~ 50 or more cells each. This process emulates tumorigenic capacity of cancer cells and formation of CSC-like clones is associated with stemness qualities. To understand whether Amx or FSS may alter mammosphere formation and stemness 3D generation of CSCs were dispergated and placed again in no adherant conditions either with the absence or presence of corresponding antibiotics (Figure 23).

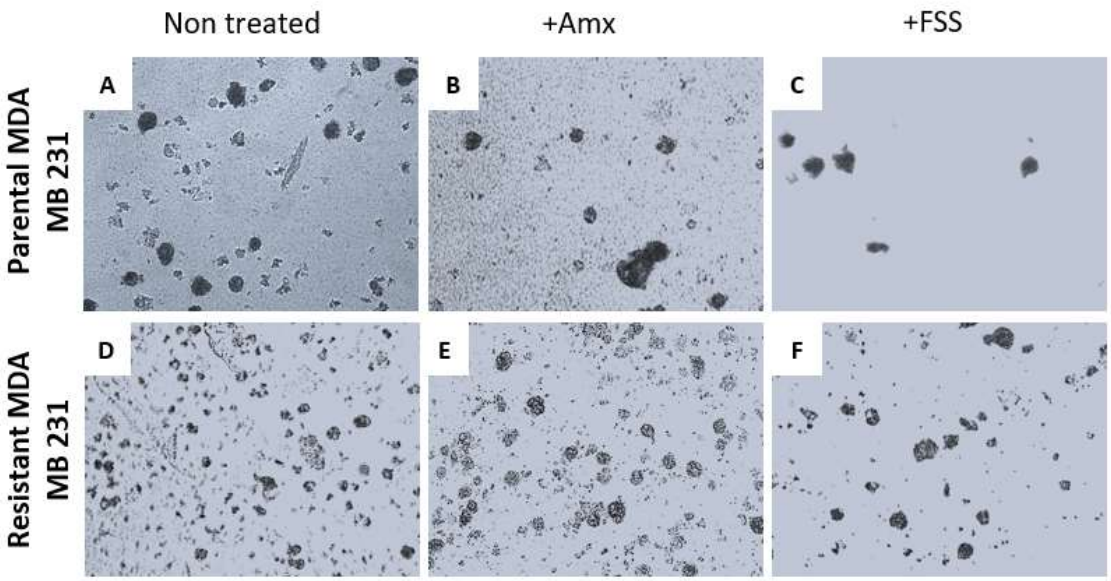

Figure 23. Analysis of mammosphere formation in the presence of antibiotics. MDA MB 231 parental (A-C) and resistant (D-F) cancer cells were used to create CSC for 3 generations. Following 4th generation, mammosphere formation assay was performed and the microscopic images were taken with 20x resolution. Similarly, the assay was done in the presence of IC20 concentrations of Amx (B,E) or FSS (C, E). Expreriments were done in quadruplicates.

Corresponsing microscopic images were manually counted. Parental CSC formed ~14 colonies while resistant CSCs formed 24 colonies in average before treatment. Amx and FSS treatment significantly inhibited mammosphere formation. In resistant cells, number of colonies decreased to 23 and 16 with Amx and FSS treatment respectively (Figure 24).

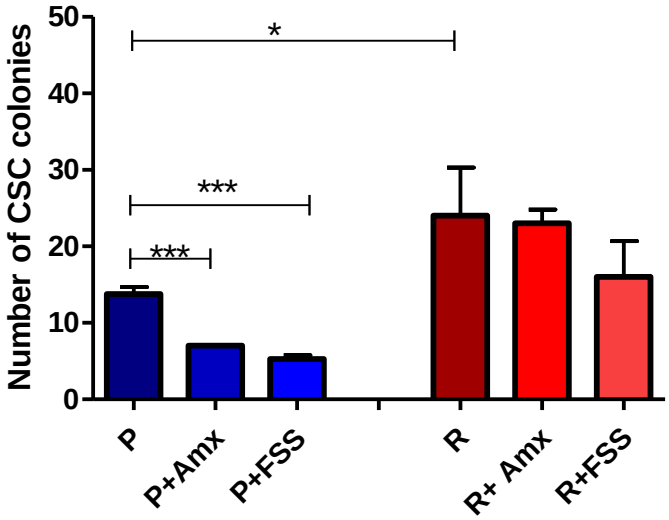

Figure 24. Antibiotics reduce mammosphere formation. The number of spheroids from microscope images (n=4) before and after treatment with Amx and FSS was counted and plotted on the graph. P- parental CSC, P+Amx :- parental CSCs with Amx treatment, P+ FSS - parental CSCs with FSS treatment, R- resistant CSC, R+Amx - resistant CSCs with Amx treatment, R+ FSS- resistant CSCs with FSS treatment, * $P \leq 0.05$, ** $P \leq 0.01$, *** $P \leq 0.001$.

4.4.4. Protein Profiling by Western Blotting

The above results demonstrate that lead antibioitcs, Amx and FSS, show increase in the OCR, tumosphere formation and MMP activities. In order to explore some underlining pathways in details, a pilot protein profiling of some selected pathways was performed through the Western blotting anaysis of three proteins: Epithelial catherin (E cadherin), a major marker of cell adhesion which low expression may correleate with increased metastasis (Mendonsa, Na, and Gumbiner 2018); UQCRC2 (cytochrome c reductase core protein 2), an OXPHOS marker representing a core protein for mitochondrial complex III (Han et al. 2019); and LC3 (microtubule-associated protein 1 light chain 3) protein as an important marker or autophagy (Cherra et al. 2010), was investigated in parental, CSC and resistant cancer cells. A weak decrease was observed in the expression of E cadherin protein after 1 day treatment with Amx and FSS both in parental and resistant cells (Figure 25, A). Expression level of E cadherin in CSC was significantly lower than in parental cells, which corroborate with the stemness properties of these cells having weak adhesion.

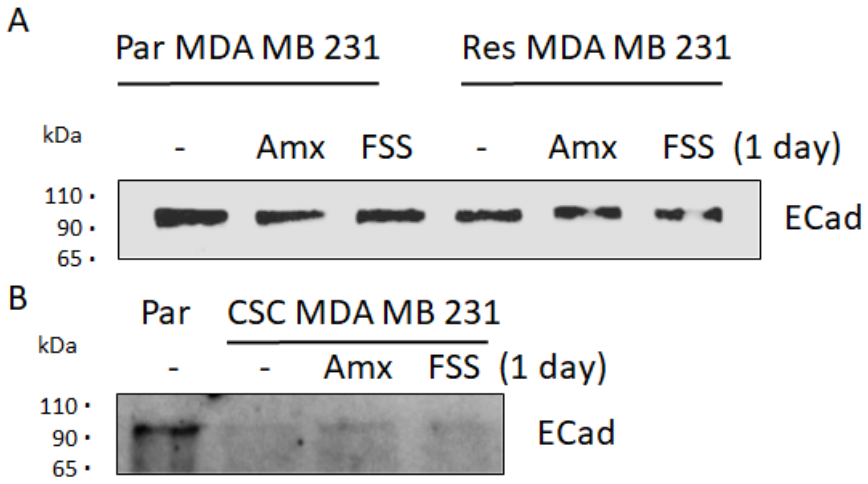

Figure 25. Expression of E Cadherin upon exposure of MDA MB 231 cancer cells to antibiotics. (A) Western Blot demonstrates a weak decrease in E Cadherin protein expression upon exposure to Amx and FSS antibiotics for 1 day on parental and resistant cancer cells. (B) The expression level of E Cadherin in resistant and even more so in cancer stem cells (CSC) is significantly lower than in parental counterparts.

UQCRC2 expression was significantly higher in resistant cells compared to parental cells (Figure 26, A). Upon treatment with Amx and FSS, a weak deline in the expression of UQCRC2 for parental and resistant cells and a strong decline for CSC was observed. (Figure 26, B).

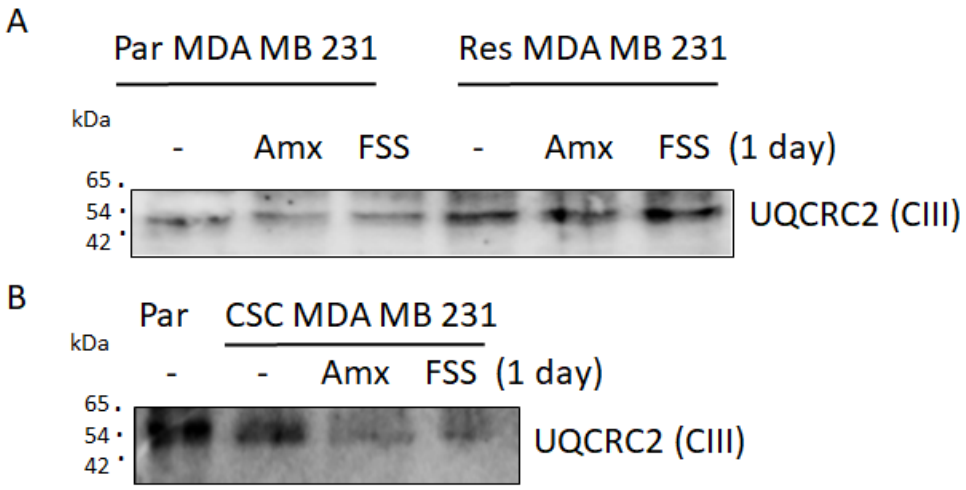

Figure 26. Expression of UQCRC2 upon exposure of MDA MB 231 cancer cells to antibiotics. Western Blot demonstrates a weak reduction in UQCRC2 respiratory complex CIII protein expression upon exposure to Amx and FSS antibiotics for 1 day on parental and resistant cancer cells (A) and a stronger inhibition of expression in stem cell cancer cells, CSC (B). The expression level of UQCRC2 in resistant cancer cells was significantly higher than in parental counterparts.

The most striking results were obtained by profiling LC3 protein expression that revealed higher ratio of LCII/ LCI correlating with enhanced autophagy. In fact, this ratio increased both in parental and resistant cells after treatment with Amx and FSS together with the largest ratio was observed in Amx treated resistant cells (Figure 27).

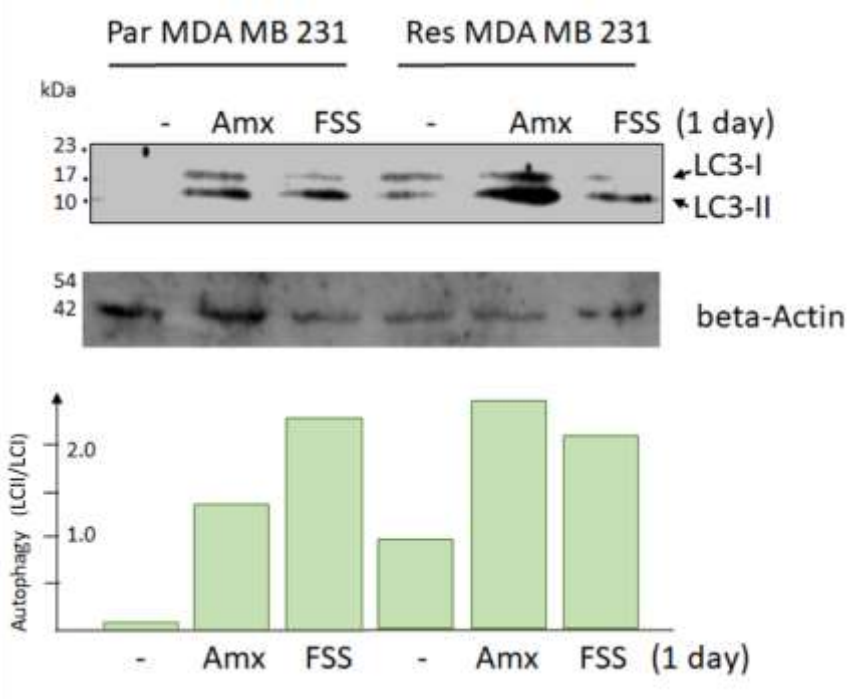

Figure 27. Treatment of cancer cells with antibiotics induces an increase in autophagy. Sensitive (parental) and resistant MDA MB 231 cells were treated with antibiotics Amx or FSS for 1 day and protein extracts were processed via Western blotting and probed for antibody representing autophagy marker LC3 (top). Loading was tested by reprobing the blot with beta-actin antibodies. The ratio of signal intensities of lipidated (LC3-II) vs. non-lipidated (LC3-I) forms shows the degree of autophagy in the cells.

5. DISCUSSION

In the current study, lead antibiotics were investigated as potential chemotherapeutic agents to overcome chemoresistance in TNBC model MDA MB 231 cells. First, cisplatin-resistant MDA MB 231 cells were established by continious exposure to a certain concentration of the drug. After preliminary experiments, IC20 of cisplatin was chosen for all subsequent treatments, as higher concentrations over long periods of times result in very few surviving cells, making them difficult to collect and analyze. After prolonged

exposure to cisplatin for several months, the development of a resistant phenotype in MDA MB 231 cells was confirmed by MTT assay, revealing a nearly twofold increase in the IC50 value and preservation of viability even at higher concentrations of cisplatin.

Initial characterisation of model cells was obtained by comparing cell morphology, replication time, and ability to adobt to the treatment.

Following the acquisition of resistance, the doubling time of cisplatin-resistant cells increased almost two times compared to their sensitive counterparts, also indicating a reduced proliferation capacity. Similar increases in doubling time have been reported in studies on mouse mammary tumors (Zhou et al. 2023) and colorectal cancer cells (Sazonova et al. 2024). In fact, cell cycle arrest is a frequently observed phenomenon in drug-resistant cancers (Hammerlindl and Schaider 2018), and it has been documented that cells can switch to a quiesent (dormant) state after acquiring resistancy (Sharma et al. 2010) . In our study, cells may alter their cell cycle dynamics to mitigate the toxic effects of cisplatin, possibly through modulation the expressionof cell cycle-related genes (Liau et al. 2017).

To characterize the resistance phenotype of MDA MB 231 cells, the colony formation ability of parental and resistant cells was also examined. Parental cells formed significantly more colonies than resistant cells. This result is not surprising in terms of the lower growth rate of the resistant cells. Similarly, the number of colonies was significantly reduced in parental cells after incubation with increased concentrations of cisplatin, while this was less so in resistant cells. In general, more metastatic cells give rise to a higher number of colonies. In our case, the results suggest that slower doubling time associated with acquired resistance of MDA MB 231 cells does not allow to form new colonies with the same rates as parental cell do.

One of the main concepts of the study was to answer a pivotal question of whether parental and resistant cells have different respiration capacity, both at the cellular and mitochondrial level. We successfully detected this difference using OCR experiments and supported it by Western blotting analysis.

When measuring OCR, baseline values were initially recorded without any intervention. At this stage, resistant cells exhibited a higher OCR compared to parental cells. Although higher initial OCR in resistant cells gives a hint about mitochondrial respiration, this result may also be related to a larger cell size and glycolysis. Therefore, ADP was injected into the oxygraph chambers to increase ADP/ATP ratio and promotoe OXPHOS. An increase in the ADP/ATP ratio is a prerequisite for the regulation of cellular respiration and an indicator of energy demand. To provide this energy, cells begin to produce ATP through OXPHOS (Nelson 2013). After the addition of ADP, OCR nearly doubled in resistant cells, while it did not change significantly in parental cells.

Although ADP is also recognized as a key regulator of the glycolytic enzyme phosphofructokinase-1 (will be tested in future work) (Nelson 2013), and its addition can also stimulate glycolysis, the decrease in oxygen levels suggests that resistant cells primarily utilize oxidative phosphorylation (OXPHOS) to meet their energy demand rather than relying on glycolysis. Introduction of FCCP further supported increased OXPHOS in resistant cells. FCCP is an uncoupler which dissipates the H+ gradient between the matrix and the inner mitochondrial membrane (Muller et al. 2019). Under normal conditions, the H+ gradient is necessary for ATP production through ATPase in mitochondria. However, FCCP enables cells to carry out mitochondrial respiration independently from the H+ gradient, making it possible to measure the maximum OCR achievable by cells (Plitzko and Loesgen 2018). Following FCCP administration, OCR peaked in resistant cells, contrasting with the relatively stable OCR observed in parental cells. Collectively, these results emphasize the higher respiratory capacity of resistant cells, which utilize predominantly OXPHOS for ATP production, compared to parental cells.

To find out how increasing OXPHOS affects cellular ATP levels and mitochondrial mass, we measured these parameters in resistant and parental cells. As anticipated, resistant cells exhibited elevated ATP levels compared to parental cells, which correlates with a notable difference in mitochondrial mass between the two cell types. A previous study suggested that increased OXPHOS levels in prolifeating cells correlate with elevated mitochondrial fusion (Yao et al. 2019). Therefore, increased mitochondrial mass in our study may be the result of mitochondrial fusion. This may take place on genomic level through the aquisition of some mutations. Indeed, mutations in the mitochondria are common situation which lead to mitochondrial (H. Chen et al. 2010; L. Chen, Winger,

and Knowlton 2014). Mitochondria of the resistant cells could get damaged upon subsequent exposure to cisplatin. When mitochondria are damaged, they can fuse with healthy mitochondria to form new, larger and healthier organnell to compensate for the damage to the damaged mitochondria. This fusion can also enhance the ability of mitochondria to OXPHOS (Youle and Van Der Bliek 2012). These results may also explain elevated OXPHOS level in resistant cells.

To discern specific components of OXPHOS actively involved in resistant and parental cells, we assessed the protein expression of mitochondrial complex III subunit UQCRC2 by Western blotting (results for other complexes are in progress) and quantified mitochondrial complex II activity using a kit. UQCRC2 is a core subunit protein of mitochondrial complex III. Our data show that resistant cells demonstrated significanly higher expression of UQRCR2 protein than parental cells. Resistant cells also showed increased mitochondrial complex II activity compared to parental cells. Although mitochondrial complex II activity was measured based on promising preliminary results obtained from cyclophosphamide-resistant MDA MB 231 cells, future investigations will also explore the activity of other mitochondrial complexes. The results suggest that mitochondrial complex II and mitochondrial complex III may contribute to OXPHOS of resistant cells. Not surprisingly, previous studies have focused on complex II and complex III to overcome drug resistance (Chu et al. 2022; Liang et al. 2015; Prochazka et al. 2013).

Since resistant and parental cancer cells differentiatially dependent on OXPHOS, this quality could be used to repurpose antibiotics to inhibit mitochondrial function in the resistant cancer phenotype, thus overcomeing drug resistant tumors. Perhaps, if antibiotics work as OXPHOS inhibitors, they could be used as a neoadjuvant chemotherapy or combination therapy along with chemo- or radiotherapy. Previous studies have demonstrated that some of the antibiotics inhibits mitochondrial biogenesis (Lamb et al. 2015), some stimulate mitochondrial disfunction (Lleonart et al. 2017), and some inhibit cancer cell growth (Esner et al. 2017). It is supported by animal experiments showing that antibioitcs, more specifically some tetracyclines, inhibit OXPHOS (Kuntz et al. 2017).

With this approach, we selected two antibiotics, Amoxicillin (sodium) and Fosmidomycin (sodium salt), to target OXPHOS and overcome drug resistance. We repeated nearly all assays in the presence of these two drugs, Amx and FSS.

We started to test activity of Amx and FSS by measuring total ATP levesl of parental and resistant cells. Our findings revealed increases ATP levels upon antibiotic treatment in all cases except for resistant cells treated with FSS. Interestingly, mitochondrial mass in both parental and resistant cells also increased following treatment with Amx and FSS. Similarly, mitochondrial complex II activity also increased in both parental and resistant cells after treatment with Amx and FSS. These results were unexpected based on concept of the study.

Although these results seem to contradict the basic logicg of the study, if we consider mitochondrial fusion under stress conditions and mutations, they are understandable. Antibiotics are are known to induce cellular stress and generate ROS (Dwyer et al. 2014; Li et al. 2021). Our results suggest that Amx and FSS likely led to cellular stress and mitochondrial damage, which further resulted in mitochondrial fusion, increased mitochondrial mass, cellular ATP, and increased complex II activity.

In this regard, when measuring OCR in parental and resistant cells using a Clark-type oxygraph, we observed higher OCR in both resistant and parental cells after Amx and FSS treatment. However, this increase in OCR could also be attributed to peroxisomes. Peroxisomes play a role in fatty acid and amino acid oxidation, lipid synthesis, and glyoxylate detoxification (Chornyi et al. 2021). All of these reactions directly or indirectly require molecular oxygen. The peroxisome utilizes molecular oxygen as a co-substrate for H_2O_2 production (Lismont, Revenco, and Fransen 2019). Therefore, the increase in OCR upon Amx and FSS treatment may be the result of peroxisomal O_2 utilization. To circumvent this issue and examine the direct effect of Amx and FSS on OXPHOS, we measured OCR in the Seahorse XF24 analyzer using mitochondrial subparticles. We observed OCR decline in resistant cells treated with IC20 Amx and FSS, while it was unchanged in parental cells. These results indicate that Amx and FSS inhibit OXPHOS in resistant cells if the mitochondria are not protected by the intact cell and are readily accessible to antibiotics.

In addition to OXPHOS, antibioitcs can affect other mechanisms. Since we observed in a wound healing assay that resistant cells have increased metastatic properties than parental cells, we wanted to investigate the effect of Amx and FSS on metastatic ability of cells. Matrix metallaproteinases play an active role in EMT during metastasis. Therefore, we measured MMP-2 and MMP-9 activity with gelatin zymography assay. Gelatin zymograpgh is not the best method to measure cellular activity of MMPs because physiological conditions are not recapitulated on the gel. However, it is usefull for understanding the presence of specific MMPs and their potential activities (Toth, Sohail, and Fridman 2012).

In this assay, we observed that pro-MMP-9 expressed more in resistant cells than in parental cells. Higher pro MMP-9 in the resistant cells confirmed metastatic potential of resistant cells. Not surprisingly, treatment with Amx and FSS decreased pro-MMP levels in both parental and resistant cells. These results suggest that Amx and FSS reduced the metastatic capacity of resistant cells, possibly by decreasing the expression of pro-MMP-9. Similar results were observed in CSCs. CSCs form spherical colonies that play an active role in metastasis. After treatment with Amx and FSS, the number of colonies of parental and resistant CSCs decreased, which correlates with decrease in the expression of pro-MMP-9

To further explore the metastatic potential of resistant and parental cells after Amx and FSS treatment, we examined E-cadherin expression using Western blot analysis. E-cadherin is a cell adhesion protein, and its low expression is associated with higher metastasis (Mendonsa, Na, and Gumbiner 2018). As expected, CSCs expressed significantly less E cadherin than parental cells. The NF-κB or STAT3 pathway may be involved in the transition from parental cells to resistant cells. Since these pathways are activated in cancer cells by interleukins, and activation of NF-κB or STAT3 leads to MMP expression and leads to the transition to EMT (Briukhovetska et al. 2021). The reduction of MMP activity by antibiotic treatment makes this statement possible: Amx and FSS may also affect the NF-κB or STAT3 pathway by activating interleukin expression, leading to a decrease in MMP activity and metastatic potential.

In addition to changes in metastatic potential, another notable finding from the Western blot analysis was the increased expression of the autophagy marker, lipidated LC3II, after treatment with Amx and FSS. From the antibiotic screening results of the study, it is

evident that Amx and FSS have higher toxicity to resistant cells. One of the primary objectives of our study was to elucidate the possible mechanisms underlying toxicity of Amx and FSS. Although Amx and FSS demonstrated inhibitory effects on OXPHOS and metastasis, they also appear to affect autophagy pathways. ROS is one of the main triggers of autophagy (Filomeni, De Zio, and Cecconi 2015). Since antibiotics act as stressors that induce ROS production, Amx and FSS possibly stimulate ROS-triggered autophagy (and most likely mitophagy) pathways. We also detected increase in the ROS level in our unpublished study performed on Artemia Salina (brine shrimp) after antibiotics treatment. This result also correlates with the increase in mitochondrial mass upon Amx and FSS treatment as described in Results. Given that damaged mitochondria are likely cleared by selective autophagy (mitophagy) or fused to preserve resistant cells, co-administration of autophagy inhibitors with Amx and FSS could potentially enhance the inhibitory activity of these antibiotics.

To summarize, in this study, we succesfully demonstrated that cisplatin-resistant MDA MB 231 cells have elevetad OXPHOS level and increased metastatic properties compared to their sensitive counterparts. Furthermore, we showed that antibiotics, Amx and FSS, have higher cytotoxic activiy against resistant cancer cells than parental cells. They also limit formation of cancer stem-like cells indicating potentially reduced metastatic capacity. The selected antibiotics exert their inhibitory activity by affecting various mechanisms including decreasing OXPHOS levels, reducing aggressive metastatic properties by decreasing MMP and E-cadherin expression and enhancing autophagy pathways.

6. CONCLUSION

Breast cancer remains a leading cause of death among women worldwide, primarily due to metastasis. Cancer stem cells (CSCs) and cancer resistant cells (CRC) play pivotal roles in metastasis, making them promising targets for therapeutic interventions to reduce cancer mortality. CSCs and CRC are resistant to chemo- and radiotherapy, thus sensitizing these subsets of cells to therapy is crucial. Therefore, in this study, we investigated the efficacy of antibiotics, specifically Amoxicillin (Amx) and Fosmidomycin sodium salt (FSS), in targeting cancer resistance through mitochondria. As a result, we conclude:

- cisplatin resistant MDA MB 231 cells differ from their sensitive parental counterparts by their morphology, higher metastatic capacity and OXPHOS-dependency;
- both Amx and FSS antibiotics demonstrated toxic effects on CRC, reducing their metastatic capacity by inhibiting MMP activity and E cadherin expression, decreasing OXPHOS and inducing autophagy pathways;
- both Amx and FSS antibiotics effectively reduced formation of CSCs.

7. BIBLIOGRAPHY

Abad, Etna et al. 2019. “Common Metabolic Pathways Implicated in Resistance to Chemotherapy Point to a Key Mitochondrial Role in Breast Cancer,.” *Molecular & Cellular Proteomics* 18(2): 231–44.

Anurag, Meenakshi et al. 2022. “Proteogenomic Markers of Chemotherapy Resistance and Response in Triple-Negative Breast Cancer.” *Cancer Discovery* 12(11): 2586–2605. /cancerdiscovery/article/12/11/2586/709984/Proteogenomic-Markers-of-Chemotherapy-Resistance (June 17, 2024).

Arps, David P. et al. 2013. “Invasive Ductal Carcinoma with Lobular Features: A Comparison Study to Invasive Ductal and Invasive Lobular Carcinomas of the Breast.” *Breast Cancer Research and Treatment* 138(3): 719–26.

Bardal, Stan K., Jason E. Waechter, and Douglas S. Martin. 2011. “Applied Pharmacology.” : 470. https://books.google.com/books/about/Applied_Pharmacology.html?hl=tr&id=nYPy70d1E50C (June 17, 2024).

Batlle, Eduard, and Hans Clevers. 2017. “Cancer Stem Cells Revisited.” *Nature Medicine* 23(10): 1124–34.

Bray Bsc, Freddie et al. 2024. “Global Cancer Statistics 2022: GLOBOCAN Estimates of Incidence and Mortality Worldwide for 36 Cancers in 185 Countries.” https://acsjournals.onlinelibrary.wiley.com/doi/10.3322/caac.21834 (June 17, 2024).

Briukhovetska, Daria et al. 2021. “Interleukins in Cancer: From Biology to Therapy.” *Nature Reviews Cancer* 21(8): 481–99. http://dx.doi.org/10.1038/s41568-021-00363-z.

Chambers, Ian et al. 2003. “Functional Expression Cloning of Nanog, a Pluripotency Sustaining Factor in Embryonic Stem Cells.” *Cell* 113(5): 643–55.

Chen, Hsiuchen et al. 2010. “Mitochondrial Fusion Is Required for Mtdna Stability in Skeletal Muscle and Tolerance of MtDNA Mutations.” *Cell* 141(2): 280–89.

Chen, Le, Allison J. Winger, and Anne A. Knowlton. 2014. “Mitochondrial Dynamic Changes in Health and Genetic Diseases.” *Molecular Biology Reports* 41(11): 7053–

62.

Cherra, Salvatore J. et al. 2010. “Regulation of the Autophagy Protein LC3 by Phosphorylation.” *Journal of Cell Biology* 190(4): 533–39.

Chinnery, Patrick Francis. 2003. “Mitochondria.” *Journal of Neurology, Neurosurgery & Psychiatry* 74(9): 1188–99.

Chornyi, Serhii et al. 2021. “Peroxisomal Metabolite and Cofactor Transport in Humans.” *Frontiers in Cell and Developmental Biology* 8(January): 1–24.

Christensen, Jon, and V. Prasad Shastri. 2015. “Matrix-Metalloproteinase-9 Is Cleaved and Activated by Cathepsin K.” *BMC Research Notes* 8(1): 1–8.

Chu, Man et al. 2022. “Targeting Cancer Stem Cells by Nutraceuticals for Cancer Therapy.” *Seminars in Cancer Biology* 85(May 2021): 234–45. https://doi.org/10.1016/j.semcancer.2021.07.008.

Cree, Ian A., and Peter Charlton. 2017. “Molecular Chess? Hallmarks of Anti-Cancer Drug Resistance.” *BMC Cancer* 17(1): 1–8. http://dx.doi.org/10.1186/s12885-016-2999-1.

Delaloge, Suzette, Seema Ahsan Khan, Jelle Wesseling, and Timothy Whelan. 2024. “Ductal Carcinoma in Situ of the Breast: Finding the Balance between Overtreatment and Undertreatment.” *Lancet (London, England)* 403(10445): 2734–46. https://pubmed.ncbi.nlm.nih.gov/38735296/ (June 30, 2024).

Dwyer, Daniel J. et al. 2014. “Antibiotics Induce Redox-Related Physi.” *Proceedings of the National Academy of Sciences of the United States of America* 111(20).

Eljack, Nasma D. et al. 2014. “Mechanisms of Cell Uptake and Toxicity of the Anticancer Drug Cisplatin.” *Metallomics : integrated biometal science* 6(11): 2126–33. https://pubmed.ncbi.nlm.nih.gov/25306996/ (June 17, 2024).

Esner, Milan, Dmitry Graifer, Matilde E. Lleonart, and Alex Lyakhovich. 2017. “Targeting Cancer Cells through Antibiotics-Induced Mitochondrial Dysfunction Requires Autophagy Inhibition.” *Cancer Letters* 384: 60–69.

Evans, Kurt W. et al. 2021. “Oxidative Phosphorylation Is a Metabolic Vulnerability in Chemotherapy-Resistant Triple-Negative Breast Cancer.” *Cancer Research* 81(21): 5572. /pmc/articles/PMC8563442/ (June 17, 2024).

Fanelli, Marilù et al. 2016. “Targeting ABCB1 and ABCC1 with Their Specific Inhibitor CBT-1® Can Overcome Drug Resistance in Osteosarcoma.” *Current cancer drug targets* 16(3): 261–74. https://pubmed.ncbi.nlm.nih.gov/26548759/ (June 17, 2024).

Filomeni, G., D. De Zio, and F. Cecconi. 2015. “Oxidative Stress and Autophagy: The

Clash between Damage and Metabolic Needs." *Cell Death and Differentiation* 22(3): 377–88.

Florea, Ana Maria, and Dietrich Büsselberg. 2011. "Cisplatin as an Anti-Tumor Drug: Cellular Mechanisms of Activity, Drug Resistance and Induced Side Effects." *Cancers* 3(1): 1351–71. https://pubmed.ncbi.nlm.nih.gov/24212665/ (June 17, 2024).

Fotakis, George, and John A. Timbrell. 2006. "In Vitro Cytotoxicity Assays: Comparison of LDH, Neutral Red, MTT and Protein Assay in Hepatoma Cell Lines Following Exposure to Cadmium Chloride." *Toxicology Letters* 160(2): 171–77.

Fukushima, Reo et al. 2018. "Overexpression of Translocation Associated Membrane Protein 2 Leading to Cancer-Associated Matrix Metalloproteinase Activation as a Putative Metastatic Factor for Human Oral Cancer." *Journal of Cancer* 9(18): 3326–33.

Gerstberger, Stefanie, Qingwen Jiang, and Karuna Ganesh. 2023. "Metastasis." *Cell* 186(8): 1564–79. https://pubmed.ncbi.nlm.nih.gov/37059065/ (June 17, 2024).

Ghosh, Sumit. 2019. "Cisplatin: The First Metal Based Anticancer Drug." *Bioorganic Chemistry* 88(March): 102925. https://doi.org/10.1016/j.bioorg.2019.102925.

Green, Douglas R. 1998. "Apoptotic Pathways: The Roads to Ruin." *Cell* 94(6): 695–98. https://pubmed.ncbi.nlm.nih.gov/9753316/ (June 17, 2024).

Hammerlindl, Heinz, and Helmut Schaider. 2018. "Tumor Cell-Intrinsic Phenotypic Plasticity Facilitates Adaptive Cellular Reprogramming Driving Acquired Drug Resistance." *Journal of Cell Communication and Signaling* 12(1): 133–41.

Han, Yingyan et al. 2019. "Ubiquinol-Cytochrome C Reductase Core Protein II Promotes Tumorigenesis by Facilitating P53 Degradation." *EBioMedicine* 40: 92–105. https://doi.org/10.1016/j.ebiom.2019.01.002.

Hanahan, Douglas, and Robert A. Weinberg. 2011. "Hallmarks of Cancer: The next Generation." *Cell* 144(5): 646–74. https://pubmed.ncbi.nlm.nih.gov/21376230/ (June 17, 2024).

Hill, David P. et al. 2019. "Cisplatin-Resistant Triple-Negative Breast Cancer Subtypes: Multiple Mechanisms of Resistance." *BMC Cancer* 19(1): 1–13.

Huang, Lei, A. Man Xu, and Wei Liu. 2015. "Transglutaminase 2 in Cancer." *American Journal of Cancer Research* 5(9): 2756. /pmc/articles/PMC4633903/ (June 17, 2024).

Irvin, William J., and Lisa A. Carey. 2008. "What Is Triple-Negative Breast Cancer?"

European Journal of Cancer 44(18): 2799–2805.

Jang, Ji Yong, Arnon Blum, Jie Liu, and Toren Finkel. 2018. "The Role of Mitochondria in Aging." *Journal of Clinical Investigation* 128(9): 3662–70.

Jeter, Collene R. et al. 2015. "Concise Review: NANOG in Cancer Stem Cells and Tumor Development: An Update and Outstanding Questions." *Stem Cells* 33(8): 2381–90.

Kelland, Lloyd. 2007. "The Resurgence of Platinum-Based Cancer Chemotherapy." *Nature reviews. Cancer* 7(8): 573–84. https://pubmed.ncbi.nlm.nih.gov/17625587/ (June 17, 2024).

Kleiner, D E, and W G Stetler-Stevenson. 1999. "Metaloproteasas de Matriz y Metástasis." *La quimioterapia y la farmacología del cáncer* 43 Suppl: S42–51.

Kumari, U., W. Ya Jun, B. Huat Bay, and A. Lyakhovich. 2014. "Evidence of Mitochondrial Dysfunction and Impaired ROS Detoxifying Machinery in Fanconi Anemia Cells." *Oncogene* 33(2): 165–72.

Kuntz, Elodie M. et al. 2017. "Targeting Mitochondrial Oxidative Phosphorylation Eradicates Therapy-Resistant Chronic Myeloid Leukemia Stem Cells." *Nature Medicine* 23(10): 1234–40.

Lagadinou, Eleni D. et al. 2013. "BCL-2 Inhibition Targets Oxidative Phosphorylation and Selectively Eradicates Quiescent Human Leukemia Stem Cells." *Cell stem cell* 12(3): 329–41. https://pubmed.ncbi.nlm.nih.gov/23333149/ (June 17, 2024).

Lamb, Rebecca et al. 2015. "Antibiotics That Target Mitochondria Effectively Eradicate Cancer Stem Cells, across Multiple Tumor Types: Treating Cancer like an Infectious Disease." *Oncotarget* 6(7): 4569. /pmc/articles/PMC4467100/ (June 17, 2024).

Lebert, J. M. et al. 2018. "Advances in the Systemic Treatment of Triple-Negative Breast Cancer." *Current oncology (Toronto, Ont.)* 25(Suppl 1): S142–50. https://pubmed.ncbi.nlm.nih.gov/29910657/ (June 17, 2024).

Lee, Kyung min et al. 2017. "MYC and MCL1 Cooperatively Promote Chemotherapy-Resistant Breast Cancer Stem Cells via Regulation of Mitochondrial Oxidative Phosphorylation." *Cell Metabolism* 26(4): 633-647.e7.

Li, Hao et al. 2021. "Reactive Oxygen Species in Pathogen Clearance: The Killing Mechanisms, the Adaption Response, and the Side Effects." *Frontiers in Microbiology* 11(February).

Liang, Desheng et al. 2015. "Enhance Cancer Cell Recognition and Overcome Drug Resistance Using Hyaluronic Acid and α-Tocopheryl Succinate Based Multifunctional Nanoparticles." *Molecular Pharmaceutics* 12(6): 2189–2202.

Liau, Brian B. et al. 2017. “Adaptive Chromatin Remodeling Drives Glioblastoma Stem Cell Plasticity and Drug Tolerance.” *Cell Stem Cell* 20(2): 233-246.e7.

Lismont, Celien, Iulia Revenco, and Marc Fransen. 2019. “Peroxisomal Hydrogen Peroxide Metabolism and Signaling in Health and Disease.” *International Journal of Molecular Sciences* 20(15).

Liu, Zhenhui et al. 2020. “Cancer Cells Display Increased Migration and Deformability in Pace with Metastatic Progression.” *FASEB Journal* 34(7): 9307–15.

Lleonart, Matilde E., Robert Grodzicki, Dmitri M. Graifer, and Alex Lyakhovich. 2017. “Mitochondrial Dysfunction and Potential Anticancer Therapy.” *Medicinal research reviews* 37(6): 1275–98. https://pubmed.ncbi.nlm.nih.gov/28682452/ (July 4, 2024).

Lu, Yun et al. 2010. “Evidence That SOX2 Overexpression Is Oncogenic in the Lung.” *PLoS ONE* 5(6).

Luo, Ming, Michael Brooks, and Max Wicha. 2015. “Epithelial-Mesenchymal Plasticity of Breast Cancer Stem Cells: Implications for Metastasis and Therapeutic Resistance.” *Current Pharmaceutical Design* 21(10): 1301–10.

Makovec, Tomaz. 2019. “Cisplatin and beyond: Molecular Mechanisms of Action and Drug Resistance Development in Cancer Chemotherapy.” *Radiology and oncology* 53(2): 148–58. https://pubmed.ncbi.nlm.nih.gov/30956230/ (June 17, 2024).

Mansoori, Behzad et al. 2017. “The Different Mechanisms of Cancer Drug Resistance: A Brief Review.” *Advanced Pharmaceutical Bulletin* 7(3): 339–48. http://dx.doi.org/10.15171/apb.2017.041.

Margulis, Lynn. 1967. “On the Origin of Mitosing Cells.” *Journal of theoretical biology* 14(3): 255–74. http://www.ncbi.nlm.nih.gov/pubmed/11541390.

Massagué, Joan, and Karuna Ganesh. 2021. “Metastasis-Initiating Cells and Ecosystems.” *Cancer discovery* 11(4): 971–94. https://pubmed.ncbi.nlm.nih.gov/33811127/ (June 17, 2024).

McGuirk, Shawn et al. 2021. “Resistance to Different Anthracycline Chemotherapeutics Elicits Distinct and Actionable Primary Metabolic Dependencies in Breast Cancer.” *eLife* 10. https://pubmed.ncbi.nlm.nih.gov/34181531/ (June 17, 2024).

Méndez-López, Luis Fernando. 2022. “Revisiting Epithelial Carcinogenesis.” *International Journal of Molecular Sciences* 23(13).

Mendiratta, Gaurav et al. 2021. “Cancer Gene Mutation Frequencies for the U.S. Population.” *Nature Communications* 12(1): 1–11. http://dx.doi.org/10.1038/s41467-021-26213-y.

Mendonsa, Alisha M., Tae Young Na, and Barry M. Gumbiner. 2018. “E-Cadherin in Contact Inhibition and Cancer.” *Oncogene* 37(35): 4769–80. http://dx.doi.org/10.1038/s41388-018-0304-2.

Michael, M., and M. M. Doherty. 2005. “Tumoral Drug Metabolism: Overview and Its Implications for Cancer Therapy.” *Journal of Clinical Oncology* 23(1): 205–29.

Mukerabigwi, Jean Felix et al. 2023. “Mitochondria-Targeting Polyprodrugs to Overcome the Drug Resistance of Cancer Cells by Self-Amplified Oxidation-Triggered Drug Release.” *Bioconjugate Chemistry* 34(2): 377–91.

Muller, Bethany et al. 2019. “Application of Extracellular Flux Analysis for Determining Mitochondrial Function in Mammalian Oocytes and Early Embryos.” *Scientific Reports* 9(1): 1–14.

Murphy, Gillian, and Thomas Crabbe. 1995. “Gelatinases A and B.” *Methods in Enzymology* 248(C): 470–84.

National Institutes of Health. 2007. “Understanding Cancer.” https://www.ncbi.nlm.nih.gov/books/NBK20362/.

Nelson, Cox. 2013. 53 Journal of Chemical Information and Modeling *Lehninger’s Principles of Biochemistry*.

Orrantia-Borunda, Erasmo et al. 2022. “Subtypes of Breast Cancer.” *Breast Cancer*: 31–42. https://www.ncbi.nlm.nih.gov/books/NBK583808/ (June 17, 2024).

Osborne, Newton G. 2008. Infectious Diseases in Obstetrics and Gynecology, Sixth Edition *Mycoplasma*.

Page-McCaw, Andrea, Andrew J. Ewald, and Zena Werb. 2007. “Matrix Metalloproteinases and the Regulation of Tissue Remodelling.” *Nature Reviews Molecular Cell Biology* 8(3): 221–33.

Pastò, Anna et al. 2014. “Cancer Stem Cells from Epithelial Ovarian Cancer Patients Privilege Oxidative Phosphorylation, and Resist Glucose Deprivation.” *Oncotarget* 5(12): 4305. /pmc/articles/PMC4147325/ (June 17, 2024).

Phi, Lan Thi Hanh et al. 2018. “Cancer Stem Cells (CSCs) in Drug Resistance and Their Therapeutic Implications in Cancer Treatment.” *Stem Cells International* 2018.

Del Pino Herrera, Adriana, and Meghan C. Ferrall-Fairbanks. 2024. “A War on Many Fronts: Cross Disciplinary Approaches for Novel Cancer Treatment Strategies.” *Frontiers in genetics* 15. https://pubmed.ncbi.nlm.nih.gov/38873108/ (June 30, 2024).

Plaks, Vicki, Niwen Kong, and Zena Werb. 2015. “The Cancer Stem Cell Niche: How

Essential Is the Niche in Regulating Stemness of Tumor Cells?" *Cell stem cell* 16(3): 225. /pmc/articles/PMC4355577/ (July 1, 2024).

Plitzko, Birte, and Sandra Loesgen. 2018. "Measurement of Oxygen Consumption Rate (OCR) and Extracellular Acidification Rate (ECAR) in Culture Cells for Assessment of the Energy Metabolism." *Bio-Protocol* 8(10): 1–13.

Prochazka, Lubomir et al. 2013. "Mitochondrial Targeting Overcomes ABCA1-Dependent Resistance of Lung Carcinoma to α-Tocopheryl Succinate." *Apoptosis* 18(3): 286–99.

Roger, Andrew J., Sergio A. Muñoz-Gómez, and Ryoma Kamikawa. 2017. "The Origin and Diversification of Mitochondria." *Current Biology* 27(21): R1177–92.

Rosenberg, B., L. Van Camp, E. B. Grimley, and A. J. Thomson. 1967. "The Inhibition of Growth or Cell Division in Escherichia Coli by Different Ionic Species of Platinum(IV) Complexes." *Journal of Biological Chemistry* 242(6): 1347–52.

Saad, Sherif Y., Tawfeeg A.O. Najjar, and Mouied Alashari. 2004. "Role of Non-Selective Adenosine Receptor Blockade and Phosphodiesterase Inhibition in Cisplatin-Induced Nephrogonadal Toxicity in Rats." *Clinical and Experimental Pharmacology and Physiology* 31(12): 862–67.

Sales Amaral, Márcia Vanessa et al. 2019. "Establishment of Drug-Resistant Cell Lines as a Model in Experimental Oncology: A Review." *Anticancer research* 39(12): 6443–55. https://pubmed.ncbi.nlm.nih.gov/31810908/ (June 17, 2024).

Sampath, Deepa et al. 2006. "Pharmacodynamics of Cytarabine Alone and in Combination with 7-Hydroxystaurosporine (UCN-01) in AML Blasts in Vitro and during a Clinical Trial." *Blood* 107(6): 2517–24.

Sazonova, Elena V. et al. 2024. "Cancer Drug Resistance: Targeting Proliferation or Programmed Cell Death." *Cells* 13(5).

Schaefer, Thorsten, and Claudia Lengerke. 2020. "SOX2 Protein Biochemistry in Stemness, Reprogramming, and Cancer: The PI3K/AKT/SOX2 Axis and Beyond." *Oncogene* 39(2): 278–92. http://dx.doi.org/10.1038/s41388-019-0997-x.

Schwitalla, Sarah et al. 2013. "Intestinal Tumorigenesis Initiated by Dedifferentiation and Acquisition of Stem-Cell-like Properties." *Cell* 152(1–2): 25–38.

Shaath, Hibah, Ramesh Elango, and Nehad M. Alajez. 2021. "Molecular Classification of Breast Cancer Utilizing Long Non-Coding RNA (LncRNA) Transcriptomes Identifies Novel Diagnostic LncRNA Panel for Triple-Negative Breast Cancer." *Cancers* 13(21). https://pubmed.ncbi.nlm.nih.gov/34771513/ (June 17, 2024).

Sharma, Sreenath V. et al. 2010. “A Chromatin-Mediated Reversible Drug-Tolerant State in Cancer Cell Subpopulations.” *Cell* 141(1): 69–80. http://dx.doi.org/10.1016/j.cell.2010.02.027.

Shibata, Masahiro, and Mohammad Obaidul Hoque. 2019. “Targeting Cancer Stem Cells: A Strategy for Effective Eradication of Cancer.” *Cancers* 11(5). /pmc/articles/PMC6562442/ (June 17, 2024).

Siegel, Rebecca L., Angela N. Giaquinto, and Ahmedin Jemal. 2024. “Cancer Statistics, 2024.” *CA: a cancer journal for clinicians* 74(1): 12–49. https://pubmed.ncbi.nlm.nih.gov/38230766/ (June 17, 2024).

Su, Chaoyue, Jianye Zhang, Yosef Yarden, and Liwu Fu. 2021. “The Key Roles of Cancer Stem Cell-Derived Extracellular Vesicles.” *Signal transduction and targeted therapy* 6(1). https://pubmed.ncbi.nlm.nih.gov/33678805/ (June 17, 2024).

Talmadge, James E., and Isaiah J. Fidler. 2010a. “AACR Centennial Series: The Biology of Cancer Metastasis: Historical Perspective.” *Cancer research* 70(14): 5649–69. https://pubmed.ncbi.nlm.nih.gov/20610625/ (June 17, 2024).

———. 2010b. “AACR Centennial Series: The Biology of Cancer Metastasis: Historical Perspective.” *Cancer Research* 70(14): 5649–69.

Testa, Ugo, Germana Castelli, and Elvira Pelosi. 2019. “Cellular and Molecular Mechanisms Underlying Prostate Cancer Development: Therapeutic Implications.” *Medicines* 6(3): 82.

Toth, Marta, Anjum Sohail, and Rafael Fridman. 2012. “Assessment of Gelatinases (MMP-2 and MMP-9) by Gelatin Zymography.” *Methods in Molecular Biology* 878: 121–35.

Townsend, Danyelle M., and Kenneth D. Tew. 2003. “The Role of Glutathione-S-Transferase in Anti-Cancer Drug Resistance.” *Oncogene* 22(47): 7369–75. https://pubmed.ncbi.nlm.nih.gov/14576844/ (June 17, 2024).

“Understanding Breast Cancer Types | Colorado’s Breast Cancer Specialists.” https://www.rockymountaincancercenters.com/breast-cancer/types-hormone-receptors (July 15, 2024).

Uslu, Cemile, Eda Kapan, and Alex Lyakhovich. 2024. “Cancer Resistance and Metastasis Are Maintained through Oxidative Phosphorylation.” *Cancer Letters* 587(October 2023): 216705. https://doi.org/10.1016/j.canlet.2024.216705.

Walcher, Lia et al. 2020. “Cancer Stem Cells—Origins and Biomarkers: Perspectives for Targeted Personalized Therapies.” *Frontiers in Immunology* 11: 539291.

www.frontiersin.org (June 17, 2024).

Wallace, Douglas C. 2012. “Mitochondria and Cancer.” *Nature Reviews Cancer* 12(10): 685–98.

Wang, Qiang et al. 2017. “Inhibition of PARP1 Activity Enhances Chemotherapeutic Efficiency in Cisplatin-Resistant Gastric Cancer Cells.” *International Journal of Biochemistry and Cell Biology* 92: 164–72. http://dx.doi.org/10.1016/j.biocel.2017.08.001.

Wang, Zhang, and Martin Wu. 2015. “An Integrated Phylogenomic Approach toward Pinpointing the Origin of Mitochondria.” *Scientific reports* 5. https://pubmed.ncbi.nlm.nih.gov/25609566/ (June 17, 2024).

Warburg, Otto, and Seigo Minami. 1923. “Versuche an Überlebendem Carcinom-Gewebe.” *Klinische Wochenschrift* 2(17): 776–77.

Van Wart, Harold E., and Henning Birkedal-Hansen. 1990. “The Cysteine Switch: A Principle of Regulation of Metalloproteinase Activity with Potential Applicability to the Entire Matrix Metalloproteinase Gene Family.” *Proceedings of the National Academy of Sciences of the United States of America* 87(14): 5578–82.

Wen, Chunjie et al. 2019. “Curcumin Reverses Doxorubicin Resistance via Inhibition the Efflux Function of ABCB4 in Doxorubicin-Resistant Breast Cancer Cells.” *Molecular Medicine Reports* 19(6): 5162. /pmc/articles/PMC6522915/ (June 17, 2024).

WHO. 2020. 4 World Health Organization Golobal Survey *Assesing National Capacity For The Prevention and Control of Noncommunicable Diseases : Report of the 2019 Global Survey*. https://www.who.int/publications/i/item/ncd-ccs-2019.

Wolff, Antonio C. et al. 2018. “Human Epidermal Growth Factor Receptor 2 Testing in Breast Cancer: American Society of Clinical Oncology/ College of American Pathologists Clinical Practice Guideline Focused Update.” *Journal of Clinical Oncology* 36(20): 2105–22.

Xu, Yibin, Ding Xue, Armand Bankhead, and Nouri Neamati. 2020. “Why All the Fuss about Oxidative Phosphorylation (OXPHOS)?” *Journal of Medicinal Chemistry* 63(23): 14276–307.

Yang, Jing et al. 2020. “Guidelines and Definitions for Research on Epithelial–Mesenchymal Transition.” *Nature Reviews Molecular Cell Biology* 21(6): 341–52.

Yao, Cong Hui et al. 2019. “Mitochondrial Fusion Supports Increased Oxidative Phosphorylation during Cell Proliferation.” *eLife* 8: 1–19.

Yin, Li, Jiang Jie Duan, Xiu Wu Bian, and Shi Cang Yu. 2020. “Triple-Negative Breast Cancer Molecular Subtyping and Treatment Progress.” *Breast cancer research : BCR* 22(1). https://pubmed.ncbi.nlm.nih.gov/32517735/ (June 17, 2024).

Youle, Richard J, and Alexander M Van Der Bliek. 2012. “Good for Discussion: Mitochondrial Fission, Fusion, and Stress.” *Science* 337(6098): 1062–65. https://www.ncbi.nlm.nih.gov/pmc/articles/PMC4762028/pdf/nihms757703.pdf.

Yousefi, Hassan et al. 2022. “A Combination of Novel NSC Small Molecule Inhibitor along with Doxorubicin Inhibits Proliferation of Triple-Negative Breast Cancer through Metabolic Reprogramming.” *Oncogene 2022 41:47* 41(47): 5076–91. https://www.nature.com/articles/s41388-022-02497-2 (June 17, 2024).

Zaal, Esther A., and Celia R. Berkers. 2018. “The Influence of Metabolism on Drug Response in Cancer.” *Frontiers in Oncology* 8(NOV): 1–15.

Zhou, Chaoyu et al. 2023. “Establishment and Characterization of a Multi-Drug Resistant Cell Line for Canine Mammary Tumors.” *Frontiers in Veterinary Science* 10.